

UNIVERSITY OF CALGARY

Kinetic Applications of a Fluorescence Probe for Free Metal Ion Analysis

by

Tanya Elizabeth Shaw

A THESIS

SUBMITTED TO THE FACULTY OF GRADUATE STUDIES
IN PARTIAL FULFILLMENT OF THE REQUIREMENTS FOR THE
DEGREE OF MASTER OF SCIENCE

DEPARTMENT OF CHEMISTRY

CALGARY, ALBERTA

MAY, 2000

© Tanya Elizabeth Shaw 2000



National Library
of Canada

Acquisitions and
Bibliographic Services

395 Wellington Street
Ottawa ON K1A 0N4
Canada

Bibliothèque nationale
du Canada

Acquisitions et
services bibliographiques

395, rue Wellington
Ottawa ON K1A 0N4
Canada

Your file *Votre référence*

Our file *Notre référence*

The author has granted a non-exclusive licence allowing the National Library of Canada to reproduce, loan, distribute or sell copies of this thesis in microform, paper or electronic formats.

The author retains ownership of the copyright in this thesis. Neither the thesis nor substantial extracts from it may be printed or otherwise reproduced without the author's permission.

L'auteur a accordé une licence non exclusive permettant à la Bibliothèque nationale du Canada de reproduire, prêter, distribuer ou vendre des copies de cette thèse sous la forme de microfiche/film, de reproduction sur papier ou sur format électronique.

L'auteur conserve la propriété du droit d'auteur qui protège cette thèse. Ni la thèse ni des extraits substantiels de celle-ci ne doivent être imprimés ou autrement reproduits sans son autorisation.

0-612-55241-1

Canada

ABSTRACT

Kinetic Applications of a Fluorescence Probe for Free Metal Ion Analysis

Tanya Elizabeth Shaw

University of Calgary, 2000

This thesis describes the development of a fluorescence quenching technique for the measurement of solution metal-ion concentrations, and a number of environmental applications. *Lucifer Yellow* fluorescent dye (LYD), selectively quenched by Cu(II), was used as a means to study the kinetic and equilibrium interactions of Cu(II) with Laurentian fulvic (LFA), and humic acids (LHA).

The stability constant, K_S for LYD-Cu(II), increased from $\log K_S=6.24$ at pH 4.1, to $\log K_S=8.60$ at pH 9.1. Binding of Cu(II) by LFA occurred too rapidly for any component rate constants to be determined. Investigations of the apparent chelation equilibrium constant for Cu(II) and LFA resulted in an average value of $\bar{K} = 2.7 \pm 0.8$ mg/L. Uptake experiments for Cu(II) by LHA at pH 6.0 suggested the presence of two fast kinetic components having rate constants of 0.19 sec^{-1} and 0.020 sec^{-1} and a much slower component was also identified at pH 8.2.

ACKNOWLEDGEMENTS

I would like to first thank my supervisor, Cooper Langford and his wife, Martha, for welcoming me to Canada back in September 1997. And thank-you Cooper, for all of the assistance and direction that you provided during this Masters thesis. I would also like to express my gratitude to David Cramb (Committee member), for the keen interest he showed in my project, and for contributions and suggestions that he made along the way.

Also, thanks to everyone in the Langford research group at the University of Calgary for your company and friendship. A special thanks to Majda Djordjevic for always being there with a smile and a friendly ear.

And finally, I'd like to thank my husband, Lawton for his support, and particularly my mum and dad back in Australia for their encouragement and continued interest in what I have been doing over the past few years.

TABLE OF CONTENTS

Approval Page	ii
Abstract	iii
Acknowledgements	iv
Table of Contents	v
List of Tables	ix
List of Figures	x
CHAPTER ONE: INTRODUCTION	1
1-1. Kinetic Speciation	1
1-2. Natural Organic Ligands	1
1-3. Metal Ion Speciation	2
1-4. Mechanistic Ambiguity	5
1-5. Determining Component Rate Constants	5
1-6. Stripping Kinetics of Copper from HA	7
1-7. Stripping Kinetics of Nickel from FA	8
1-8. Species Detection Difficulties	9
1-9. Absorption and Fluorescence Techniques	10
1-9.1 Emission and Synchronous Fluorescence Quenching	10
1-9.2 Thermal Lens Spectrometry	11
1-9.3 Indirect Fluorescence Quenching	12
1-10. Research Objectives	14

CHAPTER TWO: SELECTION AND CHARACTERISATION

OF FLUORESCENT DYE	15
2-1. Introduction	15
2-2. Experimental	16
2-2.1 Dye Selection	16
2-2.2 Preparation of Solutions	17
2-2.3 Instrumentation and Fluorescence Data Collection	18
2-2.4 Quenching of LYD Fluorescence at pH 5.6	21
2-2.5 Measurement of Absorbance Shift	22
2-2.6 Effect of pH Variation on Quenching	22
2-3. Results and Discussion	23
2-3.1 Stern-Volmer Quenching Model	23
2-3.2 S-V Upward Curvature	24
2-3.3 Modified S-V Plot	29
2-3.4 pH Effect on LYD Quenching by Copper(II)	30
2-4. Summary	34

CHAPTER THREE: SPECIATION STUDIES OF COPPER(II)

WITH FULVIC AND HUMIC ACIDS	36
3-1. Introduction	36
3-2. Experimental	37
3-2.1 Preparation of Solutions	37
3-2.2 Determinations of Solution pH	39

3-2.3	Instrumentation and Data Collection	41
3-2.4	Kinetic Uptake of Copper(II) by LFA	41
3-2.5	Apparent Chelation Equilibrium of Copper(II) with LFA	42
3-2.6	Fast Kinetic Uptake of Copper(II) by Humic Acid	44
3-2.7	Long Term Study of Copper and Humic Acid Interactions	45
3-3.	Results and Discussion	50
3-3.1	Uptake Kinetics of Copper(II) by LFA	50
3-3.2	Apparent Chelation Equilibrium of Copper(II) with LFA	52
3-3.3	Rapid Kinetic Uptake of Copper(II) by LHA	57
3-3.4	Slow Kinetic Uptake of Copper(II) by LHA	66
3-3.5	Displacement of Copper(II) from LHA	66
3-4.	Summary	70
CHAPTER FOUR: CONCLUSION AND SUGGESTIONS FOR FURTHER RESEARCH		72
4-1.	Conclusion	72
4-2.	Suggestions for Further Research	74
REFERENCES		76
APPENDICES		79

Appendix 1 - Fluorescence Excitation Spectrum for <i>Lucifer</i> <i>Yellow Dye</i>	79
Appendix 2 - Fluorescence Emission Spectrum for <i>Lucifer</i> <i>Yellow Dye</i>	80
Appendix 3 - Absorbance Spectra for LYD and Copper(II)	81
Appendix 4 - Absorbance Difference Spectrum for LYD and Cu(II)	82
Appendix 5 - Absorbance Spectra for <i>Phenol Red</i> Indicator Dye	83
Appendix 6 - Absorbance Spectra for <i>Bromocresol Purple</i> Indicator Dye	84
Appendix 7 - Absorbance Spectra for <i>Bromocresol Green</i> Indicator Dye	85

LIST OF TABLES

CHAPTER TWO

Table 2-1	Properties of <i>Lucifer Yellow</i> Dye and Experimental Implications	17
Table 2-2	Experimental Fluorimeter Settings	19
Table 2-3	Stability Constant, K_S for Static Quenching: Dependence on pH	33

CHAPTER THREE

Table 3-1	Properties of pH Indicator Dyes	39
Table 3-2	Absorption Coefficients of pH Indicator Dyes	40
Table 3-3	Solution LFA and Cu^{2+} Concentrations for Apparent Equilibrium Study	43
Table 3-4	Sample Composition for Long Term Kinetic Uptake of Copper by Humic Acid	46
Table 3-5	Sample Composition for Long Term Kinetic Displacement of Copper by Humic Acid	48

LIST OF FIGURES

CHAPTER ONE

Figure 1-1	Disjunctive and Adjunctive Reaction Schemes	6
------------	---------------------------------------------	---

CHAPTER TWO

Figure 2-1	Structure of <i>Lucifer Yellow</i> Fluorescent Dye	16
Figure 2-2	Schematic Diagram of Experimental Set-up for Fluorescence Quenching Studies	20
Figure 2-3	Stern-Volmer Plot of LYD Quenching by Cu(II) with NO_3^- and SO_4^{2-} Counter Ions	25
Figure 2-4	Combined Static and Dynamic Quenching Model	26
Figure 2-5	Temperature Variation of Fluorescence Quenching	28
Figure 2-6	Castahno and Prieto Model for Fluorescence Quenching	31
Figure 2-7	pH Dependence of Fluorescence Quenching	32
Figure 2-8	Ligand Chelation Sites for Cu(II) on LYD	34

CHAPTER THREE

Figure 3-1	Kinetic Uptake of Copper(II) by Fulvic Acid	51
Figure 3-2	Apparent Copper(II)-Fulvic Acid Equilibrium Constant, K (L/mg) Plotted Against [FA] (mg/L)	54

Figure 3-3	Apparent Copper(II)-Fulvic Acid Equilibrium Constant, K (M^{-1}) Plotted Against % Coverage of LFA Sites	56
Figure 3-4	Fluorescence Signal Recorded for the Kinetic Uptake of Copper(II) by Humic Acid (pH 6.0)	58
Figure 3-5	Kinetic Uptake of Copper(II) by Humic Acid Plotted as $[Cu^{2+}]$ Versus Time	59
Figure 3-6	Kinetic Uptake of Copper(II) by Humic Acid Plotted as $\ln([CuHA]_f - [CuHA]_t)$ Versus Time	60
Figure 3-7	Data Smoothing for Laplace Transform Analysis of Kinetic Data	62
Figure 3-8	Laplace Transform Analysis of Kinetic Data	63
Figure 3-9	Slow Kinetic Uptake of Cu(II) by Humic Acid	67
Figure 3-10	Displacement of Cu(II) from Humic Acid	69

CHAPTER 1

INTRODUCTION

1-1. Kinetic Speciation

The toxicity of metal ions to biota in natural waters has long been an area of significant environmental concern. Many studies have shown that a substantial reduction in toxicity occurs in the presence of metal ion complexing agents such as humic substances and hydrous iron oxides. The “free metal ion” hypothesis (1) was introduced to account for this effect and states that the toxicity of a metal ion is proportional to the aqua ion concentration. In order to better understand and predict the bioavailability of metal ions in the natural environment, it is important to investigate the uptake and release kinetics of the metal ion with respect to the natural complexing agents, as well as equilibrium speciation. This can illuminate the exact status of the “free metal ion” hypothesis.

1-2. Natural Organic Ligands

Humic substances are natural organic complexing agents found in the environment that originate from chemically and microbially modified plant and animal matter. They are the major organic constituents in soils and are also present in the aquatic environment. The composition of natural water systems is affected by these ligands owing to their ability to bind cations and influence the pH of the water body.

Humic substances are a complex mixture of heterogenous, polydisperse electrolytes that have molecular weights in the hundreds to tens of thousands (2). They can be subdivided into three categories based on extraction properties. *Humic acid* is the fraction that cannot be extracted into solution by aqueous sodium hydroxide. The *humic acid* fraction is base soluble but precipitates in acidic solution. The fraction that is both base and acid soluble is called *fulvic acid*.

Humic acid consists of significantly higher molecular weight polyelectrolytes than the lighter fulvic acid fraction. The effects of aggregation of the polyelectrolytes and changes in conformation appear to be important factors in metal ion binding (3). These properties are likely influenced by the pH and overall surface charge on the humic and fulvic acid polyelectrolytes, as well as hydrogen bonding and donor-acceptor interactions. Because of the mixture character, the precise structure of the humic and fulvic acids cannot be specified, but the polyelectrolytes have been shown to contain phenol carboxylate, carbohydrate and aliphatic regions, joined together by covalent bonding. It is the carbohydrate functionality that appears responsible for strongest metal ion complexation, with phenol carboxylates also participating (4,5,6).

1-3. Metal Ion Speciation Studies

To date, equilibrium studies with complexing agents have constituted the vast majority of the literature on the speciation of metal ions in natural waters. However, in situations

where the rate of uptake by biota is faster than the equilibrium can be established, these thermodynamic studies may underestimate the exposure of organisms to toxic substances. It is then important to investigate the kinetic speciation of the metal ions with respect to complexing by the humic substances.

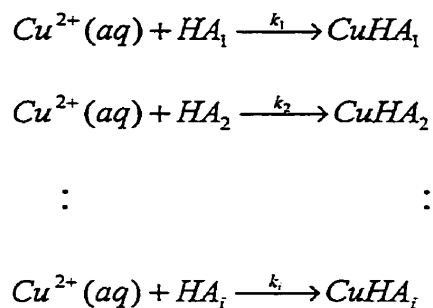
Traditional studies of kinetics have primarily involved colorimetric determinations monitoring the displacement kinetics of the metal from the humic substance (HS). A colour forming reagent specific for the metal ion of interest would be added in excess and formation of the colored metal complex would be monitored spectrophotometrically over an appropriate time period. For measurements of high sensitivity, it was important for the chromophore to have a strong binding equilibrium with the metal analyte as well as large absorptivity. The resulting release curve could then be resolved into components and the contributing species determined.

The rate of release of the complexed metal ion from the humic substance would be influenced by the relative stability of the HS-metal complex formed. Both the functional group involved in binding the metal ion as well as the local environment of the ligand may influence the stability of the complex formed and Buffle (3) has divided these secondary effects into three categories:

1. Multifunctionality of the complexing sites and different electronic and steric environments

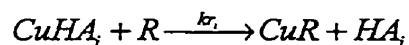
2. Conformation affecting the shape and accessibility of binding sites – influenced by the extent of hydration and hydrogen bonding as well as any bridging metal groups.
3. Polyelectrolyte properties influenced by ionic strength, pH and the degree of binding site occupation.

For copper(II) binding to humic acid (HA), the following set of competing reactions may be established.



In the above scheme, HA_1 and $\text{HA}_2 \dots \text{HA}_i$ represent separable classes of humic acid metal binding sites with rates of copper(II) uptake of k_1 and $k_2 \dots k_i$ respectively.

The displacement reactions could be similarly represented as



where R represents the colorimetric reagent and kr_i is the rate of release of copper from the humic substance. Providing the colorimetric reagent is in significant excess and the formation of monitored complex is rapid, pseudo first order kinetics will result.

1-4. Mechanistic Ambiguity

The purpose of the experiments described above is to determine the release kinetics of bound metal ions from the humic substance. However, in many cases the results are uncertain owing to the intrinsic mechanistic ambiguity of the formation of the chromophoric-metal complex. It is possible that the attacking complexing agent may strongly influence the metal release kinetics by following an adjunctive (7) pathway (Figure 1-1). In this situation, the chromophoric ligand will actually strip the metal from the humic substance, rather than binding only with the released aqueous metal ion. In a disjunctive mechanism, the release of the metal ion from the humic substance will be the rate determining step, and the uptake of free metal ion from the solution by the chromophoric compound will then be rapid, allowing the rate of release from the humic substance to be determined (Figure 1-1).

1-5. Determining Component Rate Constants

There are a number of possible methods for obtaining pseudo first-order rate constants from multicomponent systems. The Guggenheim method involves plotting differences in $\log(\text{concentration})$ against time, over a fixed time interval. Initial estimates of rate constants are calculated from linear regions of the plot where a single component is assumed to dominate (8). The relative concentrations of the individual components can then be determined from the intercept values.

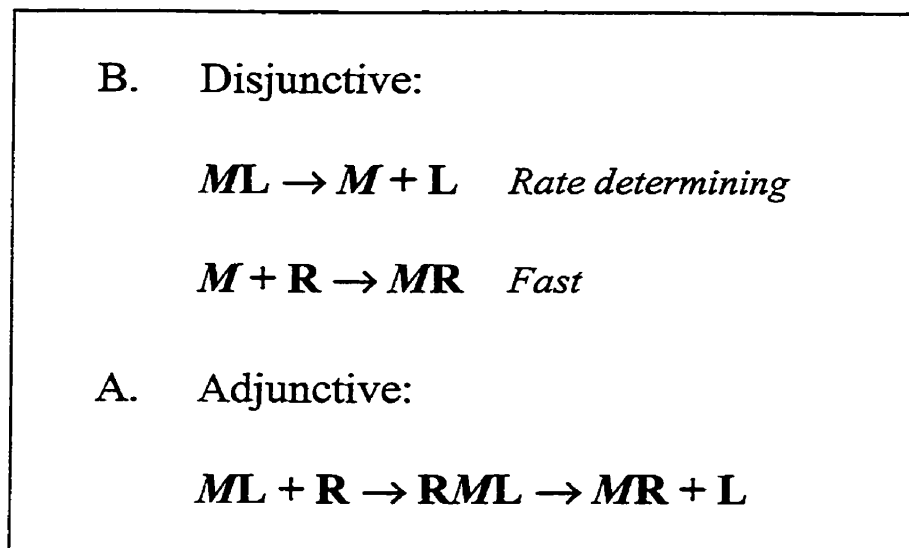


Figure 1-1. Reaction schemes depicting disjunctive (A) and adjunctive (B) reaction pathways for the detection of metal ion, M release from the binding site of a humic substance chelation site, L via the formation of a detectable metal complex, MR with a colorimetric ligand, R .

In 1983, Shuman and co-workers (9,10) introduced a method for determining component rate constants, that used a numerical approximation of a Laplace transform, derived from Equation 1.1.

$$C(t) = \sum_i C(0,i) \exp(-k_i t) \quad (1.1)$$

$C(t)$ is the concentration of HA or FA complexes with the metal ion with respect to time, t and k_i is the rate constant for the reaction of the metal with the i th species. Replacing the summation in the above equation by an integral, yields Equation 1.2 and the first and second derivatives of $C(t)$ give second-order approximate solutions to $H(k)$.

$$C(t) = S \int H(k) \exp(-kt) d[\ln k] \quad (1.2)$$

$$S = \frac{4C(t)}{\sum C(0,i)} \quad (1.3)$$

$$H(k) = \frac{d^2 C(t)}{d(\ln t)^2} - \frac{dC(t)}{d(\ln t)} \quad (1.4)$$

A plot of $H(k)$ against $\ln t$ results in a series of peaks that correspond to kinetically distinguishable components and there will be a distribution of rate constants around $\ln t$ peak values. Furthermore, the peak area will reflect the relative concentration of complexes.

1-6. Stripping Kinetics of Copper from HA

In 1996 Bonifazi, Pant and Langford (11) reported the kinetic speciation of Cu^{2+} bound to humic acid. The stripping kinetics were studied spectrophotometrically by complexation of copper with the chromophore PHTTT to form the detectable species $\text{Cu}(\text{PHTTT})_3$. The copper and humic acid solutions were equilibrated for 24 hours in the dark to allow the copper to bind to the humic acid, after which the PHTTT was added.

Complete copper reaction with PHTTT was observed and 84% of the Cu-HA complexes were determined to be highly labile, reacting within the mixing time (1.5 sec). As humic acid polyelectrolyte mixtures exist as colloidal water swollen gels, it was postulated that Cu^{2+} bound to sites inside the HA took longer to diffuse out, thus accounting for the fraction of copper (greater than 10%) with a reduced rate of release. The middle and slow components were found by the Laplace transform method to have rate constants of $0.093 \pm 0.013 \text{ sec}^{-1}$ and $0.0077 \pm 0.0008 \text{ sec}^{-1}$ respectively. Two discrete rate constants were consistently found for a number of ligand/metal ratios and two pH values.

1-7. Stripping Kinetics of Nickel from FA

A similar investigation of the speciation of nickel (II) bound to a fulvic acid was undertaken by Lavigne, Langford and Mak (12) in 1987. Aqueous nickel (II) was bound by fulvic acid in solutions equilibrated for 24 hours in the dark at pH 4, 5 and 6.4. An excess of 4-(2-pyridylazo)resorcinol (PAR) was then added to form the stable complex NiPAR that was monitored colorimetrically. For samples initially equilibrated at pH 4 and 5, 100% of the Ni^{2+} was recovered by complexation with PAR after 24 hours. At pH 6.4, 40% of the Ni^{2+} remained bound to the fulvic acid in this time and required ten days for complete release. Four kinetic species were consistently found via the method of approximate Laplace transform, with rate constants equal to 0.67, 0.15, 0.021 and 0.0026s^{-1} .

1-8. Species Detection Difficulties

Most of the studies so far have taken place in the laboratory environment with chemically extracted and purified samples from the natural environment, or laboratory synthesised polymeric colloidal compounds. When the intention is to model the natural environment, these do not represent realistic conditions. Field studies are hampered by the extremely low concentrations of metal ions of interest in the natural environment and insufficient analytical sensitivity of measurement. Often solutions must be preconcentrated before analysis which may cause redistribution of the trace metal and misleading speciation results. In natural fresh water systems, copper ranges in concentration from $10^{-8.5}$ M to $10^{-6.2}$ M and the concentration is even lower in sea water ($10^{-9.2}$ M to $10^{-8.2}$ M) (13). As the fish LC_{50} for copper are reached at concentrations of around 10^{-7} M (14), it is critical to employ sensitive detection methods when modeling these systems.

The choice of a suitable analytical method for investigations of kinetic and equilibrium speciation is limited owing to the extreme detection limits required. Most of the speciation studies that have been conducted in the past represent conditions of thermodynamic equilibrium (14), and may not constitute the most relevant information in a dynamic aquatic system. Many of the most sensitive techniques of analysis available, such as electrothermal AAS and inductively coupled plasma spectroscopy, allow only total metal concentrations to be determined. Anodic stripping voltammetry (ASV) and ion selective electrode (ISE) techniques offer low detection limits, however ASV may be

subject to adsorption and equilibria shift problems (14) and ISE is vulnerable to interferences related to the chemical environment and the presence of other ions. The humic substances are notably likely to adsorb at the electrode surfaces.

1-9. Absorption and Fluorescence Techniques

1-9.1. Emission and Synchronous Fluorescence Quenching

Fluorescence techniques have the advantage of both selectivity and sensitivity and have been used in a number of studies related to natural systems. Humic substances exhibit weak fluorescence into the visible region that is quenched upon binding metal cations. This property has been used to determine the binding equilibrium between a metal cation and humic substances, by monitoring the metal ion quenching of humic substance fluorescence, and was first introduced by Saar and Weber in 1980 (15).

A critical assumption of the method, was that quenching was directly proportional to the free ligand concentration, and this assumption was not found to be valid. Humic substances are a mixture of heterogeneous polyelectrolytes, and the humic fluorophores would be unevenly distributed throughout the mixture. There may also be metal binding sites that are shielded from the fluorophore, that would contribute little or no quenching. Emission and synchronous fluorescence measurements performed by Cook and Langford (16) using Laurentian fulvic acid (LFA) confirmed that the relationship between the

fraction of LFA sites occupied and the extent of quenching by the metal ion was non-linear.

1-9.2. Thermal Lens Spectrometry

Thermal lens spectrometry (TLS) is a technique that is based on absorption and offers high selectivity and sensitivity of measurement (17). A laser beam with a radial Gaussian intensity profile is focussed onto an absorbing analyte leading to electronic excitation of the analyte. Non-radiative relaxation of this excited complex leads to local heating of the solvent and a refractive index gradient. This refractive index gradient forms the “thermal lens” and a coaxial probe laser beam is passed through the sample. The analyte concentration is determined from the change in probe beam profile at the detector, which is reflected by a change in peak intensity at the centre of that profile.

TLS has the advantage of high sensitivity that may be enhanced by increasing the power of the pump laser beam. The signal should also be relatively insensitive to light scattering by small particles, which may interfere in regular absorbance measurements, as it relies directly on the heat produced following absorbance and not the amount of transmitted energy. Rate constants have been obtained to 2-3 significant figures, for test reactions of the bromination of acetone, from an overall absorbance change of < 0.003 (17).

TLS has been applied to the kinetic analysis of Cu(II) bound to hydrous ferric oxides and appears to be a promising technique for the study of kinetic speciation of metal ions with humic substances (17). The detection limit for Cu(II) was lower than 10^{-8} M, well below the fish LC_{50} for copper and close to the minimum natural freshwater Cu(II) concentration.

However, the technique does have some disadvantages. Larger particles (such as aggregated colloidal humic acids) may produce heterogeneous absorbances that cause high noise levels, and would need to be removed. Langford and Gutzman (17) also report that the rate coefficients that are determined are parameters of the experiment and not of the sample, however for simple mechanisms it may be possible to make a connection to related rate constants in natural systems. Furthermore, owing to the size, complexity, and cost of the TLS instruments, they are impractical for use in the field and a simpler technique is sought.

1-9.3. Indirect Fluorescence Quenching

Recent biochemical studies described by Kalsbeck and Thorpe (18) involved the use of a negatively charged fluorescent complex ($Pt_2(pop)_4^{4-}$), quenched by metal ions, for investigating the interaction of metal ions with DNA. As DNA molecules are large polyanions, interaction or chelation of the negatively charged fluorescent probe and DNA is expected to be negligible. In this way, the dynamic quenching of the fluorescent probe

could serve as a direct indicator of the concentration of free metal ions in solution and provide a means for determining the fraction of metal bound to DNA.

As humic and fulvic acids are also large polyanions at the pH of natural waters, Cook and Langford (19) recently proposed a similar methodology for investigating the binding characteristics of metal ions with humic substances, by monitoring free solution metal ion concentrations via fluorescence quenching. This would remove the ambiguity inherent in colorimetric complexation techniques where either an adjunctive or disjunctive mechanism may be followed by the complexing ligand, and provide a straightforward method of analysis.

It was proposed that a suitable anionic, fluorescent dye could be chosen that would be selectively and dynamically quenched by the ion of interest, thereby providing a sensitive and unambiguous means for studying kinetic and equilibrium speciation. Preliminary studies using the fluorescent probe *Lucifer Yellow* dye and copper(II) showed agreement with Stern-Volmer models and detection limits for free copper in the sub-micromolar range (19). The simplicity of the fluorescence instrumentation may also facilitate the development of a field technique.

1-10. Research Objectives

The overall research objective of this work was to evaluate the technique of indirect fluorescence quenching for studying the interaction of metal ions with humic and fulvic acids. The specific goals of the project are detailed below.

- (1) Select a fluorescent dye (*Lucifer Yellow*) and then characterize the quenching behaviour of the dye with respect to aqueous copper(II).
- (2) Generate a reliable calibration curve relating fluorescence quenching to concentration of free copper(II).
- (3) Use the indirect quenching method to study the equilibrium and kinetic speciation of aqueous copper(II) with humic and fulvic acids.
- (4) Discuss the advantages and limitations of the method and its suitability for use in the field.

CHAPTER 2

SELECTION AND CHARACTERISATION OF FLUORESCENT DYE

2-1. Introduction

In order to study the equilibrium and kinetic speciation of copper(II) with humic and fulvic acids, a commercial fluorescent dye was desired, that would serve as an indicator of “free” (unbound) copper(II) in solution. Humic and fulvic acids are large, soluble organic polyanions found in natural freshwater systems, and are involved in binding metal ions. The ideal dye would be predictably quenched by $\text{Cu}^{2+}(\text{aq})$ according to the Stern-Volmer relationship (20) and would satisfy the following requirements:

- high sensitivity to quenching by aqueous copper(II)
- water soluble over a wide range of pH values
- stable in aqueous solutions over the duration of measurements (up to 1 week)
- negatively charged, to prevent interaction with humic and fulvic acids by electrostatic repulsion
- an absorbance maximum > 350 nm, to avoid significant absorption by humic and fulvic acids (2)

This chapter describes the selection and characterization of a the *Lucifer Yellow* fluorescent dye. Quenching of the dye's fluorescence by aqueous copper(II) was investigated as a function of pH and temperature, and a reliable method of calibration was sought for the determination of free Cu^{2+} concentrations.

2-2. Experimental

2-2.1 Dye Selection

The fluorescent dye selected for this purpose was *Lucifer Yellow* (Molecular Probes), hereby referred to as LYD (Figure 2-1). Properties of the dye and relevant implications are listed in Table 2-1.

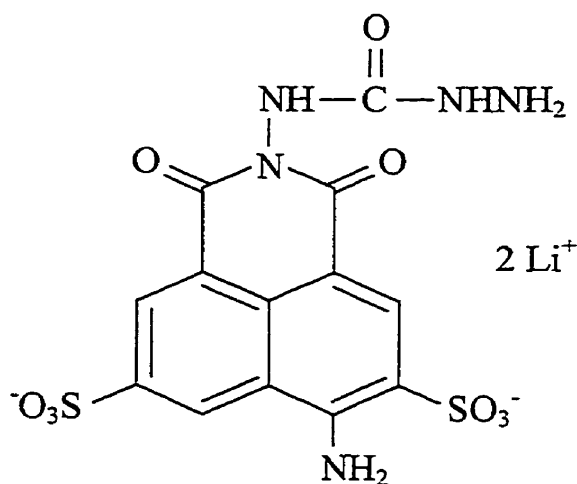


Figure 2-1. Structure of the fluorescent dye *Lucifer Yellow* (Molecular Probes), 1H-Benz[de]isoquinoline-5,8-disulfonic acid, 6-amino-2-[(hydrazinocarbonyl)amino]-2,3-dihydro-1,3-dioxo-, dilithium salt.

Table 2-1. Properties of *Lucifer Yellow Dye* and Experimental Implications

Dye Property	Experimental Implication
Double negative charge	Electrostatic repulsion should prevent interaction or binding with the humic or fulvic acid polyanions in solution
Water soluble at all pH values	Allows investigation over a natural freshwater pH range.
Reasonably stable in solution if protected from light	Allows long analysis timeframes.
Absorbance maximum at 428 nm	Humic and fulvic acid absorbance and subsequent fluorescence should be minimal (21)
Molar extinction coefficient of 12 000 L mol ⁻¹ cm ⁻¹	Strong absorbance and fluorescence signals should result. Quenching by Cu ²⁺ should allow quantitative detection of the copper to sub-micromolar concentrations.
Emission maximum at 537 nm	Fluorescence emission from humic and fulvic acids should be minimal at this wavelength (21) and little absorbance of emitted light should occur.

2-2.2 Preparation of Solutions

All solutions were prepared in Millipore Milli-Q deionized water from ACS reagents. A 0.26 mM solution of the dye was prepared by dissolving 6.0 mg of LYD (Molecular Probes) in 50.00 mL of deionized water. The solution was immediately transferred to a

Nalgene storage bottle, wrapped in foil, and stored in the dark. Aliquots of 10 - 20 μL of LYD were subsequently used in experimental work. A P20 Gilson pipette was used for these additions and was calibrated to dispense $20.0 \pm 0.2 \mu\text{L}$ (95% confidence limit).

Aqueous solutions of 30.1 mM copper sulphate were prepared in deionized water (pH 5.6) from $\text{CuSO}_4 \cdot 5\text{H}_2\text{O}$ (BDH) and diluted to give 1.500 mM, 0.150 mM, 0.015 mM and 0.014 mM $\text{Cu}^{2+}(\text{aq})$. A $\text{Cu}^{2+}(\text{aq})$ 0.014 mM solution was similarly prepared from $\text{Cu}(\text{NO}_3)_2 \cdot 2\frac{1}{2}\text{H}_2\text{O}$ (BDH). The solutions were immediately transferred to Nalgene bottles for storage.

Solutions of 0.1 M, 0.01 M NaOH (BDH) and HCl (BDH) were also prepared in deionized water and used for pH adjustments.

2-2.3 Instrumentation and Fluorescence Data Collection

An HP-8452A photodiode array UV-Vis spectrometer was used for absorbance measurements. A Perkin-Elmer 650-10S Fluorescence Spectrofluorimeter with a 150 Watt Xenon lamp was used for all fluorescence measurements and typical instrumental parameters for fluorescence quenching studies are listed in Table 2-2.

Table 2-2. Experimental Fluorimeter Settings

Parameter	Setting
Excitation wavelength, (slit width)	428 nm (8 nm)
Emission wavelength, (slit width)	537 nm (8 nm)
Range (sensitivity)	0.3
PM Gain	LOW
Response	NORMAL
Mode	NORMAL

The settings displayed in Table 2 were used in all fluorescence quenching experiments following extensive parameter optimization studies. Excitation and emission spectra of 0.87 μM LYD were recorded at a scan rate of 60 nm per minute and are displayed in Appendix 1 and 2.

A schematic diagram depicting the experimental set-up is shown in Figure 2. Light at the an excitation wavelength (428 nm) was incident on a sample cell (> 2 mL) surrounded by a water cooled jacket (8-12 $^{\circ}\text{C}$). Fluorescent emissions (at 537 nm) were collected by a photomultiplier tube at an angle of 90 degrees to the incoming beam. The analogue input was in the form nn.nnnnn in volts, with a sample rate of 10 Hz. An analogue to digital converter connected the fluorimeter to a computer. Fluorescence data with arbitrary units (0 – 1.4) were stored as a text file, recorded continuously against time in one second

intervals. Quicklog PC V2.3.1 (Strawberry Tree Inc.) software was used in the collection of data.

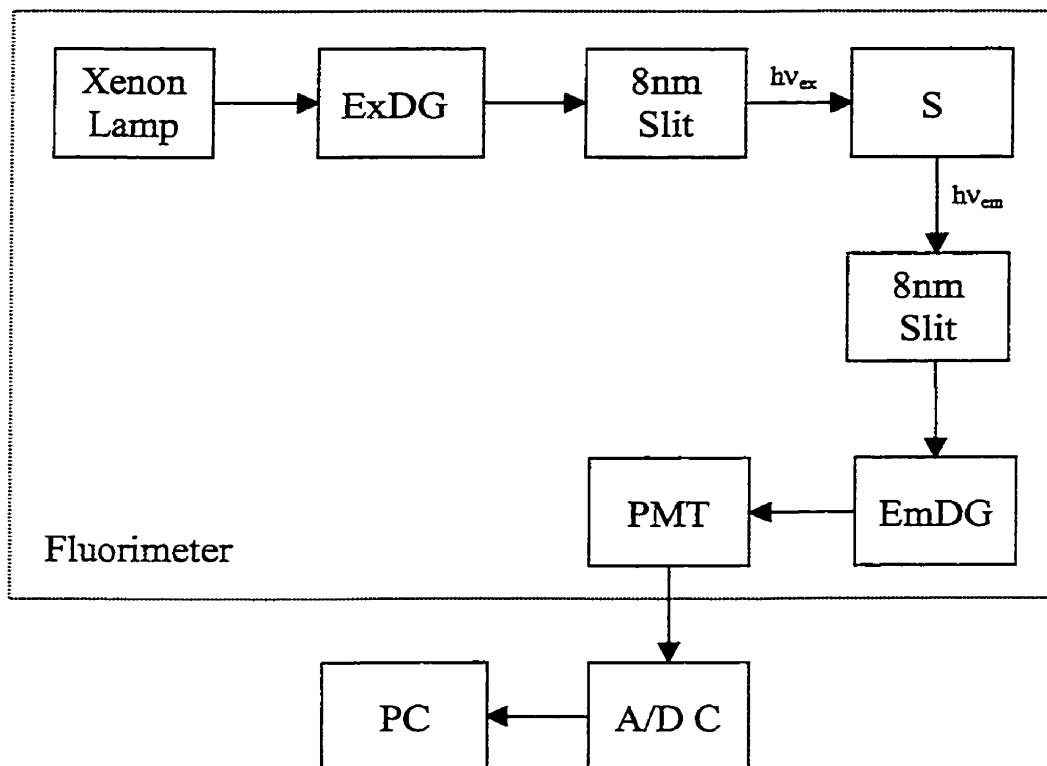


Figure 2-2. Schematic diagram of experimental set-up for fluorescence quenching studies. ExDG and EmDG represent diffraction gratings for the selection of excitation (ex) and emission (em) wavelengths respectively. PMT is a photomultiplier tube, A/D C is the analog to digital converter and PC is a personal computer.

2-2.4 Quenching of LYD Fluorescence at pH 5.6

The quenching of LYD fluorescence by $\text{Cu}^{2+}(\text{aq})$ (nitrate and sulfate counter ions) at pH 5.6 and 10 ± 2 °C was investigated in the following manner. Deionized water was used to adjust the fluorimeter PMT signal to zero. A 20 μL aliquot of 0.26 mM LYD solution was added to 3.00 mL of deionized water, followed by a total of six successive 40 μL additions of 14.0 μM $\text{CuSO}_4(\text{aq})$. The contents of the cell were mixed well by rapid inversion following each addition and the fluorescence was monitored until a constant (less than 1% signal change/min) signal was obtained. A similar experiment was performed using 14.0 μM $\text{Cu}(\text{NO}_3)_2(\text{aq})$.

The fluorescence signal of the LYD solution in the absence of copper(II) was regarded as the initial intensity I_0 and the quenched fluorescence signals were designated I . The data were plotted according to the Stern-Volmer relationship (20), as I_0/I against $[\text{Cu}^{2+}]_{\text{T}}$, the total concentration of copper(II) in the solution. The data were also plotted according to a relationship derived by Castanho and Prieto (22) as $I.[\text{Cu}^{2+}]_{\text{T}}/(I_0 - I)$ versus I/I_0 .

The above experiment using CuSO_4 as the quenching agent was repeated at pH 5.6, at a temperature of 27 ± 2 °C.

2-2.5 Measurement of Absorbance Shift

Absorbance spectra of solutions of LYD (11.9 μM) alone, $\text{Cu}^{2+}(\text{aq})$ (1.51 mM) alone, and a solution containing both LYD and Cu^{2+} (11.9 μM , 1.51 mM) were recorded over the wavelength range 180 – 820 nm (Appendix 3) and labeled as “LY”, “Cu” and “LY,Cu” respectively. An absorbance difference spectrum was then determined according to Equation 2.1 and displayed in Appendix 4.

$$\Delta A = ("LY"+"Cu") - ("LY,Cu") \quad (2.1)$$

2-2.6 Effect of pH Variation on Quenching

Millipore Milli Q deionized water was adjusted to various pH values (pH 3.1, 4.2, 5.2, 6.1, 6.9, 8.1, 9.1, 10.0) as measured by a Varian pH meter, by the dropwise addition of 0.1 M and 0.01 M solutions of HCl and NaOH to continuously stirred solutions. The PMT signal was zeroed with 3.00mL of the deionized water (pH 3.1) and a 20 μL aliquot of 0.26 mM LYD solution was then added. A total of six successive 40 μL additions of 14.0 μM CuSO_4 (aq) were made. The contents of the cell were mixed well by rapid inversion following each addition and the fluorescence was monitored until a constant (less than 1% signal change/min) signal was obtained. The process was then repeated for solutions of each listed pH.

2-3. Results and Discussion

2-3.1 Stern-Volmer Quenching Model

There are two main processes through which a fluorophore may be quenched. The quencher may either collide with the fluorophore in the excited state via diffusion, in a process called *dynamic* quenching, or a non-fluorescent complex may be formed between the fluorophore and quencher, producing *static* quenching (20). Equation 2.2 below describes the Stern-Volmer (20) relationship for dynamic quenching.

$$\frac{I_0}{I} = 1 + k_q \tau_0 [Q] \quad (2.2)$$

I_0	fluorescence intensity in the absence of quencher
I	fluorescence intensity in the presence of quencher
k_q	bimolecular quenching rate constant
τ_0	fluorescence lifetime of the fluorophore in the absence of quencher
$[Q]$	concentration of quencher in solution

A similar relationship exists for static quenching (Equation 2.3), and it is derived from the stability constant (K_S) for fluorophore-quencher complex formation (Equation 2.4).

$$\frac{I_0}{I} = 1 + K_S [Q] \quad (2.3)$$

$$K_s = \frac{[F-Q]}{[F][Q]} \quad (2.4)$$

$[F-Q]$ concentration of fluorophore-quencher complex

$[F]$ concentration of free fluorophore

A Stern-Volmer plot of I_0/I against the concentration of quencher $[Q]$ should generate a linear plot from either quenching mechanism. Quenching results at pH 5.6 (10 ± 2 °C) for LYD by $\text{Cu}^{2+}(\text{aq})$ (nitrate and sulfate) were plotted according to this relationship in Figure 2-3. The result showed clearly that the choice of anion did not interfere with the quenching process as the two curves overlaid one another. Copper sulfate solutions were used in all further quenching experiments.

2-3.2 S-V Upward Curvature

There was clear upward curvature of the plot (Figure 2-3) suggesting that the simple Stern-Volmer relationship did not adequately describe the data. Such upward curvature can often be attributed to a combination of dynamic and static quenching (20) and the relationship is described by Equation 2.5.

$$\frac{I_0}{I} = (1 + k_q \tau_0 [Q])(1 + K_s [Q]) \quad (2.5)$$

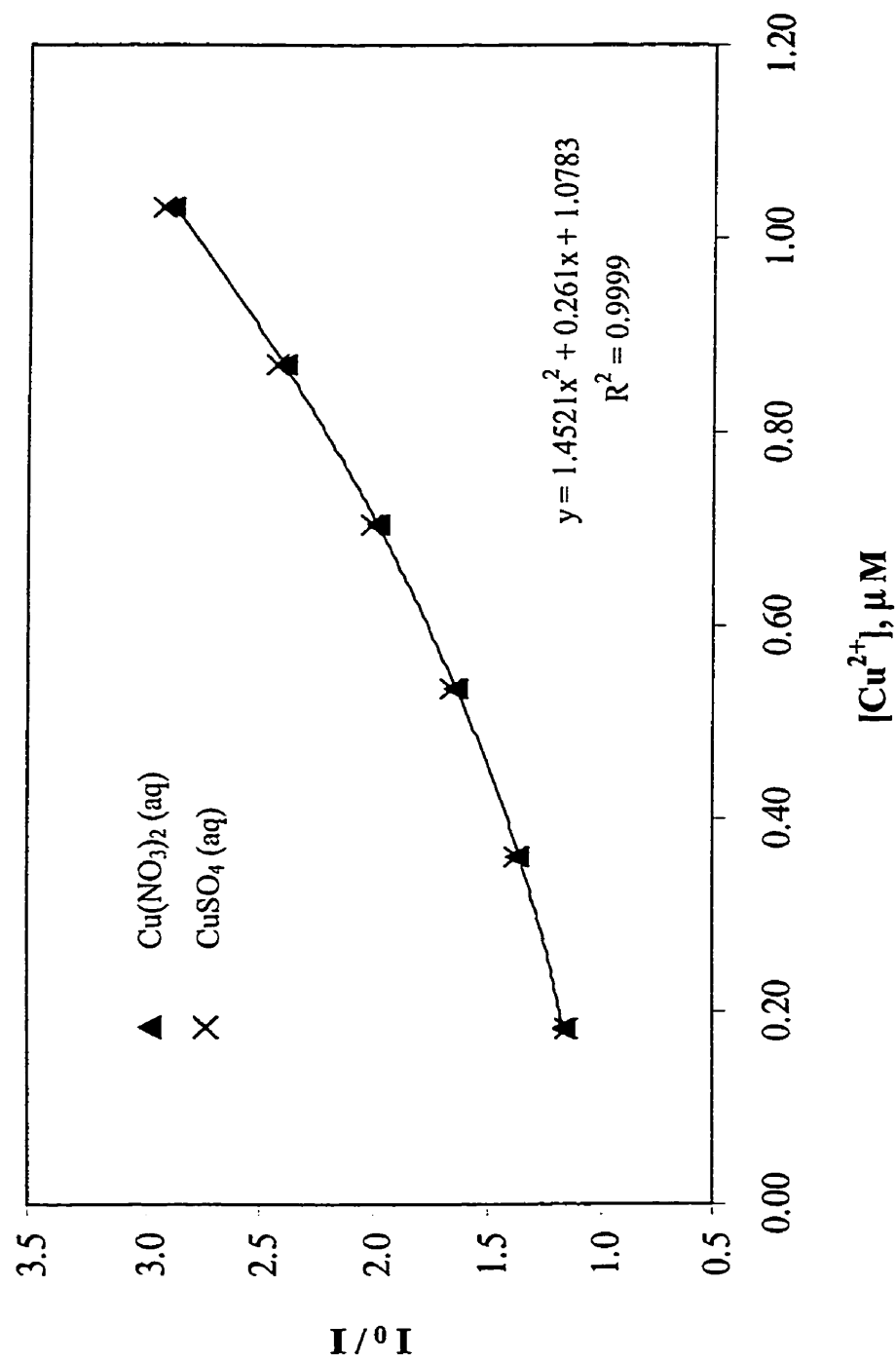


Figure 2-3. A Stern-Volmer plot depicting the quenching of 1.74 μM LYD solution (pH 5.6, 10 ± 2 $^\circ\text{C}$) by $\text{Cu}(\text{II})$ (aq) (nitrate and sulfate counter ions). A quadratic trendline was fit to the data and the equation of the line and coefficient of determination are shown.

In this case, a plot of $(I_0/I-1)/[Q]$ against $[Q]$ would result in a straight line with a slope equal to $k_q\tau_0K_S$ and an intercept of $k_q\tau_0 + K_S$. The quenching data from Figure 2-3 were plotted in this manner (Figure 2-4) and approximated by a straight line by least squares fitting ($R^2 = 0.980$). A combination of static and dynamic quenching did not appear to represent the quenching mechanism, as evidenced by the poor linear fit in Figure 2-4.

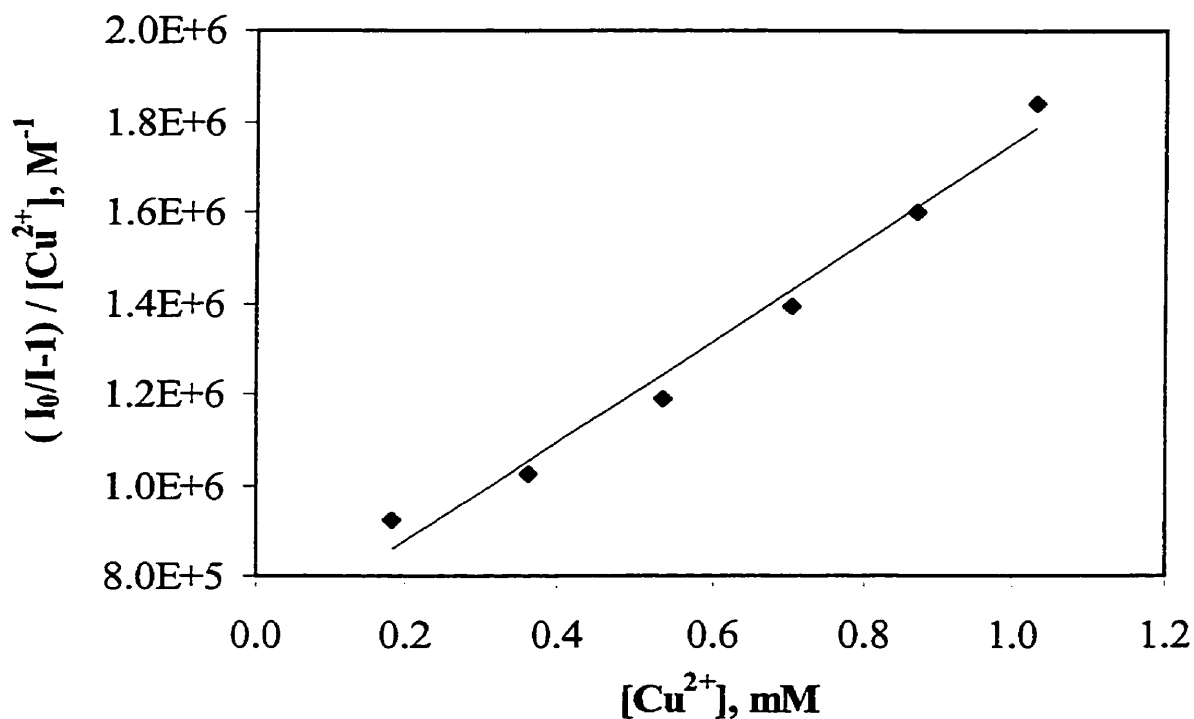


Figure 2-4. The quenching of 1.74 μM LYD solution (pH 5.6, 10 ± 2 °C) by CuSO_4 (aq), plotted according to the model for static and dynamic quenching combined (Equation 2.5). $[\text{Cu}^{2+}]$ represents the total concentration of copper(II) added.

Another common explanation of S-V upward curvature relates to the “sphere of action” effect (22). In this case, the static component of quenching results from the presence of quenching agent in the near vicinity of the dye at the time of excitation rather than complexation. Within the sphere of action, the probability of quenching is unity (22).

However, the sphere of action effect will be noticeable only for high concentrations of quencher (22). As the copper(II) concentration was in the sub-micromolar range, the effect was disregarded for this work.

Effect of Temperature

The rate of diffusion would increase with temperature, leading to greater dynamic quenching, however the temperature dependence of diffusion is weak. In comparison, the temperature dependence of equilibration ($\Delta H^\circ \neq 0$) may be significant and exponential thus any significant static quenching might dominate. At higher temperature the static complex could be *destabilized* and the overall magnitude of quenching decreased.

In order to differentiate between a predominantly static or dynamic quenching mechanism, the LYD-Cu²⁺ quenching experiment was performed at two different temperatures ($T_1=10 \pm 2$ °C, $T_2=27 \pm 2$ °C). The results of the temperature comparison are shown in Figure 2-5. As the quenching ratio I_0/I decreased substantially for

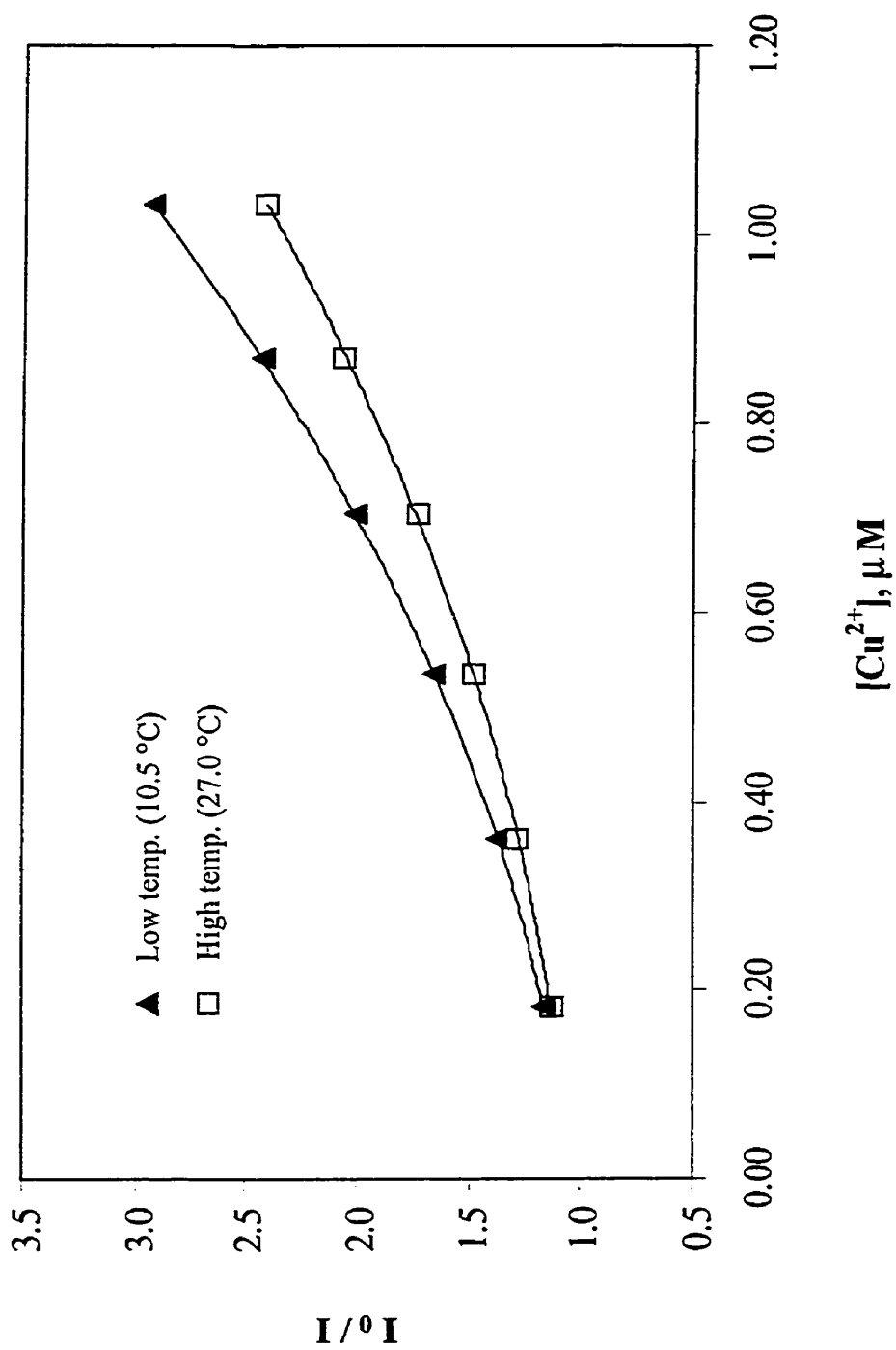


Figure 2-5. *Temperature Variation of Quenching.* Stern-Volmer plots depicting the quenching of 1.74 μM LYD solution (pH 5.6) by Cu(II) (aq) at 10.5 °C and at 27.0 °C. Quadratic trendlines have been fitted to the data.

increasing temperature, it suggested that the quenching mechanism for $\text{Cu}^{2+}(\text{aq})$ acting on LYD was predominantly *static*.

Absorbance Difference Spectrum

A slight shift in the absorbance spectrum of a solution containing both LYD and copper(II) was observed, when compared to the sum of individual spectra for LYD and Cu(II) alone (Appendix 3). This could be seen more clearly when plotted as an absorbance difference spectrum (Appendix 4) and supported a static fluorescence quenching mechanism.

2-3.2 Modified S-V Plot

The S-V model for static quenching assumes that the free and total quencher concentrations are approximately equal, $[Q] \approx [Q]_{\text{T}}$. This assumption would be valid for systems that had a small stability constant for static quenching (K_{S}) and for cases where the total concentration of quencher was far greater than the fluorophore concentration, $[Q]_{\text{T}} \gg [F]$ (22). As the concentrations of LYD and Cu^{2+} were close to 1 μM and 0.1 - 1 μM respectively, it was likely that the S-V assumptions were violated.

Castanho and Prieto (22) have recently derived a model to account for the changing concentrations of dye and quencher. The relationship is shown below (Equation 2.6, 2.7).

$$\frac{I_0}{I} = 1 + \frac{K_s}{\frac{[FQ]}{[Q]} - 1} [Q]_T \quad (2.6)$$

$$[Q]_T = [Q] + [FQ] \quad (2.7)$$

Equation 2.6 shows that purely static quenching can lead to upward curvature of S-V plots. Combining $I_0/I = [F]_0/[F]$, $[F]_T = [F] + [FQ]$ and Equations 2.4 and 2.6, the relationship was rewritten in the following form (Equation 2.8).

$$\frac{I[Q]_T}{I_0 - I} = \frac{1}{K_s} + [F]_T \frac{I}{I_0} \quad (2.8)$$

For quenching data represented by this model, a plot of $I[Q]_T / (I_0 - I)$ against I/I_0 would be linear with an intercept equal to $1/K_s$ and a slope equivalent to $[F]_T$. Figure 2-6 depicts LYD quenched at pH 5.6 ($10 \pm 2^\circ\text{C}$) by Cu^{2+} and plotted according to this relationship. The linearity of the data demonstrated the suitability of the model for the LYD-copper(II) system. This reliable calibration was applied to all further LYD- Cu^{2+} quenching studies and consistently resulted in a linear fit.

2-3.4 pH Effect on LYD Quenching by Copper(II)

The results of the pH study on copper(II) quenching of LYD are shown in Figure 2-7 and

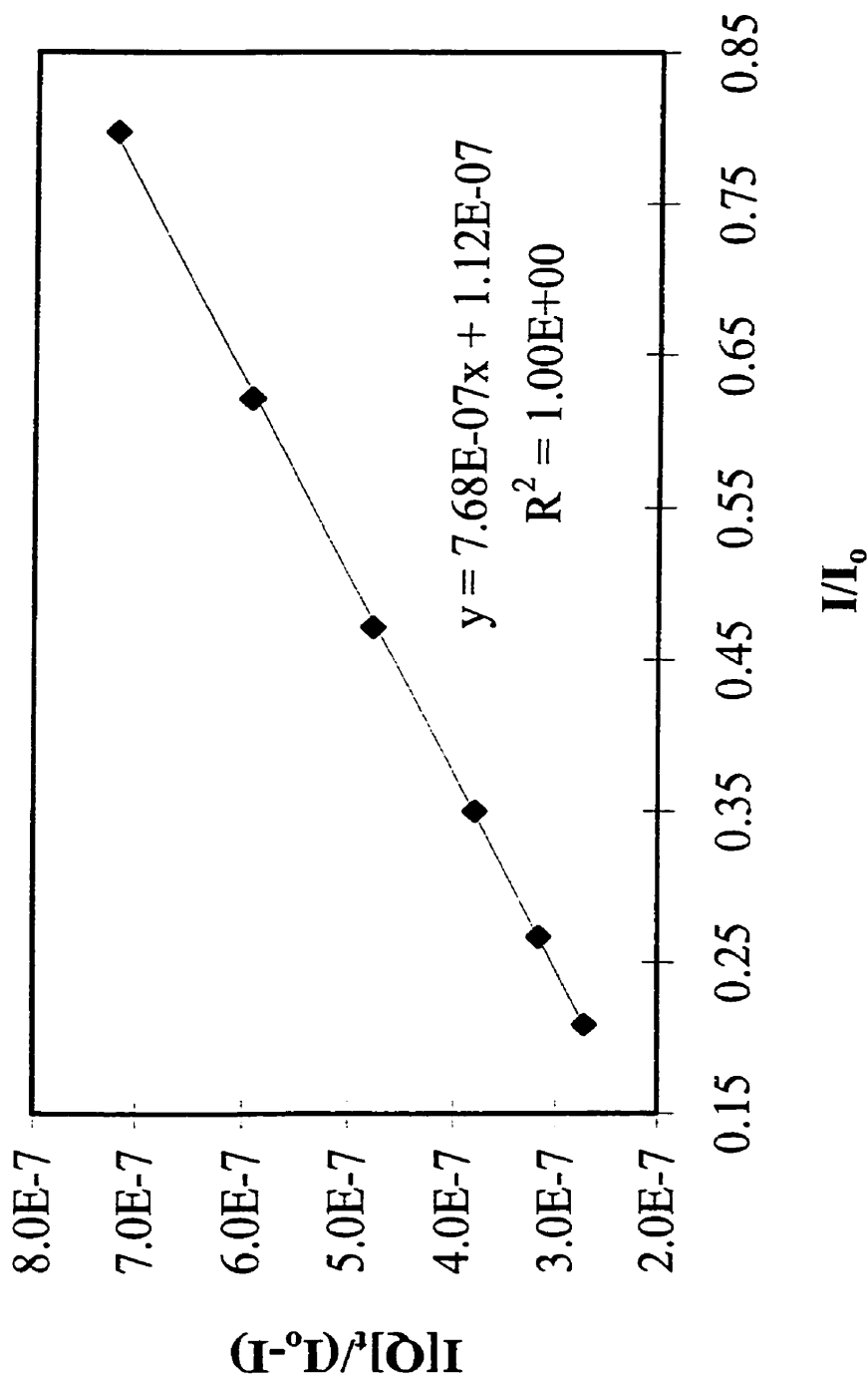


Figure 2-6. Castanho and Prieto model plot of fluorescence quenching data. A solution of 1.74 μM LYD solution (pH 5.6, 10 ± 2 $^\circ\text{C}$) quenched by Cu(II). A quadratic trendline was fit to the data and the equation of the line and correlation coefficient are shown.

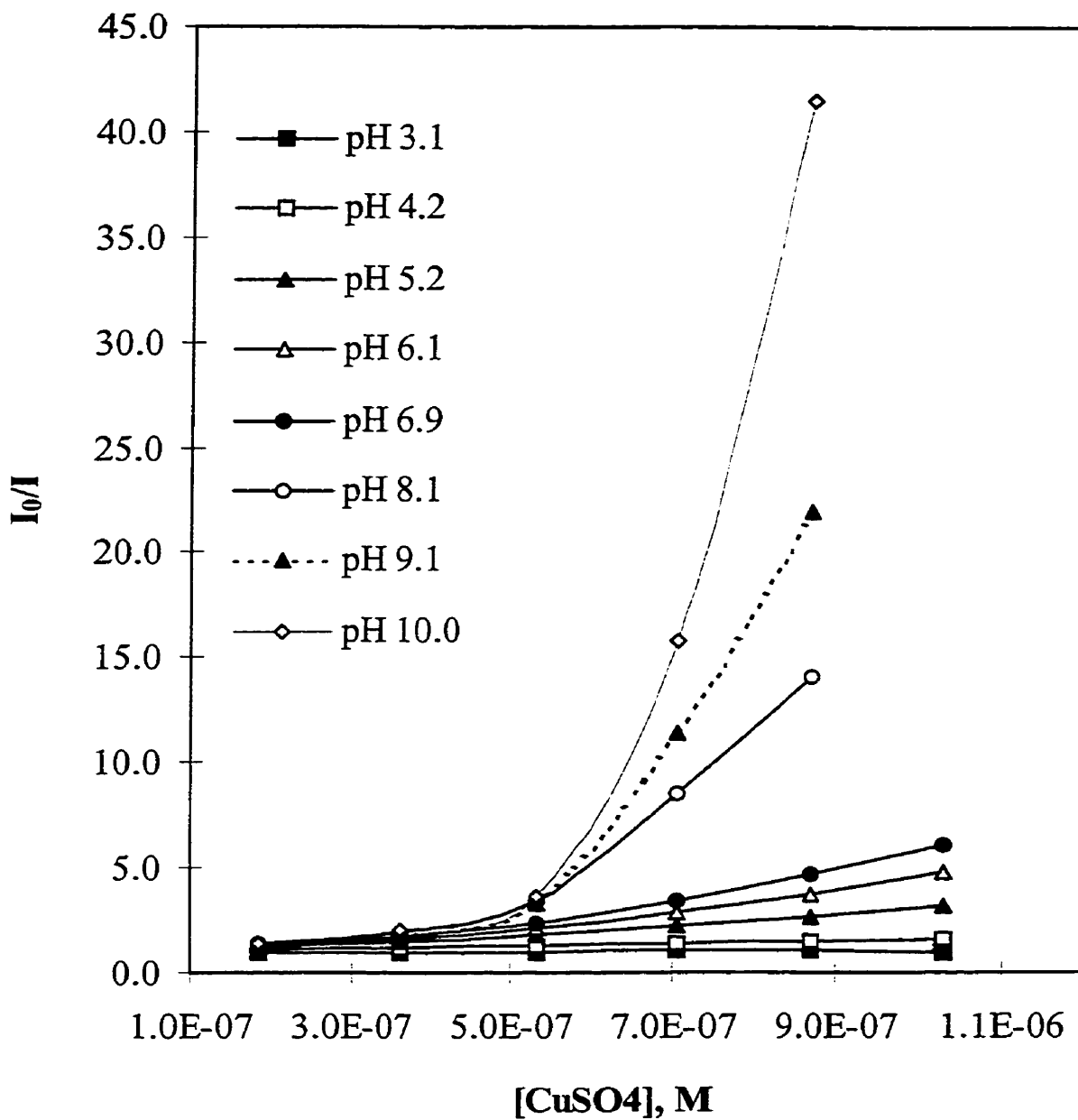


Figure 2-7. pH Dependence of Fluorescence Quenching. A Stern-Volmer plot depicting the variation in fluorescence quenching of 1.74 μ M LYD solution by Cu^{2+} over a pH range of 3.1 to 10.0.

it can be seen there was a significant increase in quenching with increasing pH. At the lowest pH (3.1), there was minimal quenching and insufficient sensitivity to determine K_S . When the remaining curves were plotted according to Equation 2.8 linear calibration curves were generated. The calculated stability constants for static quenching are listed in Table 2-3.

Table 2-3. Stability constant K_S for static quenching: Dependence on pH

pH	logK_S
4.1	6.24
5.2	6.66
6.1	6.95
6.9	7.23
8.1	7.75
9.1	8.60
10.0	8.00

The most highly favored ligand binding site for Cu^{2+} with LYD would probably have been the formation of a five-membered ring as depicted in Figure 2-8. Decreasing pH would likely result in increased protonation of the terminal amine group as shown, thus

rendering the binding site less accessible to Cu^{2+} . The apparent decrease in K_S at high pH may be due to copper hydrolysis and the formation of binuclear metal hydroxide ions.

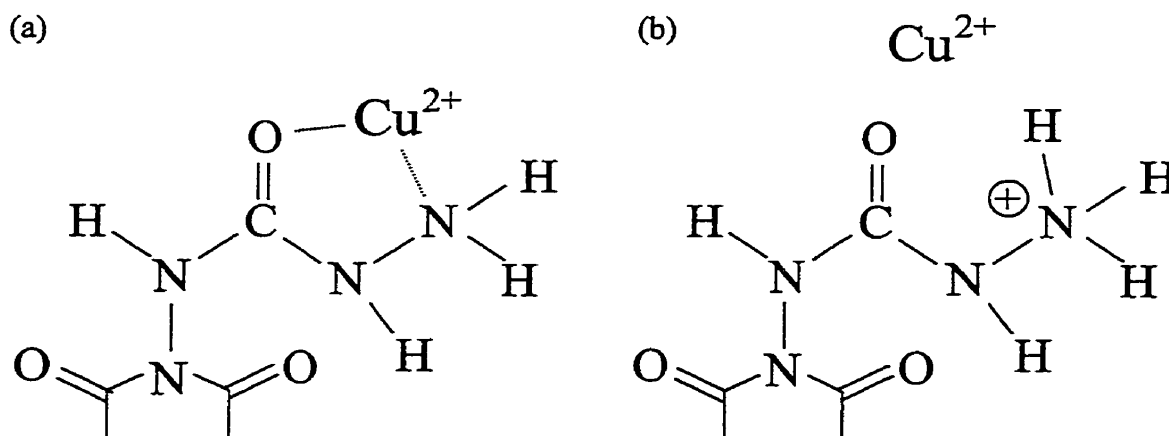


Figure 2-8. Predicted ligand chelation site for hydrated copper(II) with LYD at (a) high pH and reduced site accessibility at (b) low pH.

2-4. Summary

The fluorescent dye *Lucifer Yellow* (Molecular Probes), LYD was selected for use as an indicator of “free” copper(II) in solution. The dye had favorable spectroscopic and solubility properties, negative charge and sensitivity to quenching by aqueous copper(II). The quenching behavior of the LYD was investigated with respect to Cu^{2+} and a non-linear Stern-Volmer relationship resulted.

Decreased quenching at a higher temperature and a slight shift in the absorbance spectrum indicated a predominantly static quenching mechanism and this was explained by a relationship derived by Castanho and Prieto (22). A linear calibration curve was obtained which yielded the stability constant for static quenching, K_S .

The value of $\log K_S$ was determined to be highly dependent upon pH and increased from 6.24 (at pH 4.1) to 8.60 (at pH 9.1). Below pH 4, there was insufficient quenching to be detected and above pH 9, the magnitude of K_S decreased, possibly due to the hydrolysis of copper and formation of hydroxyl bridged dinuclear species.

Thus the LYD was found to be predictably quenched by aqueous copper(II) via a static quenching mechanism, in a highly temperature and pH dependent process.

CHAPTER 3

SPECIATION STUDIES OF COPPER(II) WITH FULVIC AND HUMIC ACIDS

3-1 Introduction

As stated previously, humic and fulvic acids are large heterogeneous polyelectrolytes that play an important role in the natural aquatic ecosystem. They are capable of binding metal cations, thereby reducing the free metal ion concentration and related toxicity to aquatic organisms. For this reason, it is important to understand the dynamic speciation of the metal ions with humic substances.

Many current methods of analysis either suffer from a lack of sensitivity or produce ambiguous results. A technique of analysis is sought, that would allow the measurement of humic substances and metal ions, at concentrations representative of the natural environment. The use of a fluorescent dye, selectively quenched by a metal ion of interest, as an indirect probe of free metal ion concentration, has the potential to become a valuable tool for meaningful environmentally studies of kinetic speciation.

This chapter describes the use of Lucifer Yellow fluorescent dye, quenched by Cu^{2+} , as a tool for the investigation of copper(II) speciation with fulvic and humic acids. The rapid rate of uptake and apparent equilibrium of copper(II) with fulvic acid was analysed and

compared to the slower rate of uptake by humic acid. A longer timeframe study of Cu^{2+} and LHA interactions was also performed.

3-2 Experimental

3-2.1 Preparation of Solutions

LYD and Copper(II) Solutions

All solutions were prepared in Millipore Milli-Q deionized water. A 0.26 mM solution of Lucifer Yellow dye was prepared as described in Chapter 2 (Section 2-2.2). Aqueous solutions of 30.1 mM copper sulphate were freshly prepared in deionized water (pH 5.6) from $\text{CuSO}_4 \cdot 5\text{H}_2\text{O}$ (BDH) and diluted to give 1.500 mM, 0.150 mM, 0.014 mM $\text{Cu}^{2+}(\text{aq})$. The solutions were immediately transferred to Nalgene bottles for storage.

Laurentian Fulvic Acid Solutions

Laurentian fulvic acid (LFA) had been extracted from a podzol soil of the Laurentian Forest Preserve of Laval University (Quebec) and had been previously been purified and prepared according to references 23 and 24. A 560 mg/L solution of LFA was prepared by dissolving 0.0280 ± 0.0005 g LFA in 50 mL of deionized water. This solution was then diluted to give 150, 50, 25, 12.5, 6.0, 2.0 and 0.5 mg/L LFA (pH 5.60). All solutions were transferred immediately to Nalgene bottles and stored in the dark.

Humic Acid Solutions

The humic acid (LHA) sample was prepared in the Langford Research Laboratories at the University of Calgary from a podzol soil of the Laurentian Forest Preserve of Laval University (Quebec) and extracted and purified by Aldo Bruccoleri according to procedures outlined in references 23 and 24. A 400 mg/L solution of LHA was prepared by dissolving 0.0103 ± 0.0005 g LHA in 25.00 mL of deionized water at pH 9.9. A 392 mg/L LHA solution at pH 11 was similarly prepared. This solution was then diluted and the pH adjusted to 8.25 to give a final LHA concentration of 8.8 mg/L.

Both the LFA and LHA had been well characterised in terms of elemental composition, NMR and FTIR spectra and metal ion and acid-base titration curves (25, 26, 27, 28, 29).

Acid, Base and pH Indicator Dye Solutions

Adjustments of pH were made with sodium hydroxide (0.1, 0.01 M) and sulfuric acid (0.1, 0.01, 0.0025 M). As humic substances are capable of adsorbing to the surface of a pH electrode and may interfere with readings, pH indicator dyes were employed to obtain accurate measurements of solution pH. The solution absorbance, calculated dye concentration and absorption coefficient could be used to determine the solution pH over the range pH 3.8 – 8.2 as described in the following section. The dyes were Phenol Red, Bromocresol Purple and Bromocresol Green (Sigma-Aldrich), all 0.04 wt % (400 mg/L) in aqueous solution, and their characteristic color changes are listed in Table 3-1. The

wavelength of maximum absorbance for the conjugate base and acid forms of the dye are listed as λ_{abs1} and λ_{abs2} respectively.

Table 3-1. Properties of pH Indicator Dyes

pH Indicator Dye	λ_{abs1} nm	λ_{abs2} nm	pK _a	Effective pH Range (Dye Colour)	
Phenol Red	558	432	7.81	pH 6.8 (yellow)	pH 8.2 (red)
Bromocresol Purple	588	432	6.12	pH 5.2 (yellow-green)	pH 6.8 (purple)
Bromocresol Green	618	446	4.66	pH 3.8 (yellow)	pH 5.4 (blue)

3-2.2 Determinations of Solution pH

Table 3-1 shows that each pH indicator dye displayed two main absorbance peaks given by λ_{abs1} and λ_{abs2} . In order to determine the coefficients of absorption for the conjugate acid and base forms of the dye, the absorbance of each dye was measured at a pH that was at least 2 units above and below the pK_a value. The resulting spectra are displayed in Appendices 5-7.

The absorption coefficients, ϵ were then calculated from the Beer-Lambert Law (Equation 3.1), where the path length, l was equal to 1.00 cm and the concentration of the dye, c was 7.84 mg/L. The absorbance, A was given by the maximum peak height at the respective wavelength of maximum absorbance. The calculated absorption coefficients for the conjugate acid, ϵ_{acid} and base forms, ϵ_{base} are listed in Table 3-2.

$$A = \epsilon cl \quad (3.1)$$

Table 3-2. Absorption Coefficients of pH Indicator Dyes

pH Indicator Dye	$\epsilon_{\text{base}} (\lambda_{\text{abs1}})$ $\text{L mg}^{-1} \text{cm}^{-1}$	$\epsilon_{\text{acid}} (\lambda_{\text{abs2}})$ $\text{L mg}^{-1} \text{cm}^{-1}$
Phenol Red	0.159 (588nm)	0.0601 (432 nm)
Bromocresol Purple	0.129 (588 nm)	0.0458 (432 nm)
Bromocresol Green	0.0658 (618 nm)	0.0284 (466 nm)

The absorbance of the conjugate base was typically stronger than the acid form, therefore this peak value was used to calculate the concentration of base, $[B]$ present in solution. As the total concentration of dye in the solution, $[D]_T$ was known, the conjugate acid concentration, $[A]$ ($= [D]_T - [B]$) was found by difference. Calculations based on the peak absorbance of the conjugate acid were used as a checking mechanism. The

experimental solution pH was then determined using the Henderson-Hasselbalch relationship (30), Equation 3.2.

$$pH = pK_a + \log \frac{[B]}{[A]} \quad (3.2)$$

3-2.3 Instrumentation and Data Collection

Fluorescence measurements were performed on a Perkin Elmer 650-10S fluorescence spectrofluorimeter and the instrumental parameters were the same as those used in dye characterisation and calibration experiments. See Chapter Two, Table 2-2 for the experimental fluorimeter settings. All absorbance measurements were performed on an HP-8452A photodiode array UV-Vis spectrometer as per Chapter Two.

3-2.4 Kinetic Uptake of Copper(II) by LFA

The kinetic uptake of copper(II) by Laurentian fulvic acid at pH 5.6 and 10 ± 2 °C was investigated. Deionised water was used to adjust the PMT signal to zero. A 20 μ L aliquot of 0.26 mM LYD solution was added to 2.00 mL of deionised water, and the fluorescence monitored to ensure a constant emission signal. A 50 - 300 μ L aliquot of 14 μ M Cu^{2+} was then added and mixed rapidly by inversion, resulting in significant quenching of the LYD fluorescence. After 2 minutes of equilibration time, 1.00 mL of

LFA solution (0.5 – 150 mg/L) was added and the fluorescent signal monitored for a further 10 minutes.

3-2.5 Apparent Chelation Equilibrium of Copper(II) with LFA

To investigate the apparent chelation equilibration of Cu^{2+} with LFA at pH 5.6, twenty solutions of varying concentrations were analysed by fluorescence measurements. The concentration of LFA and copper(II) ranged from 0.5 – 50 mg/L and 9.9×10^{-7} – 7.9×10^{-5} M respectively (See Table 3-3). The fluorescence of each LFA solution concentration in the absence of LYD or copper(II) was recorded as I_{LFA} . Following a 20 μL addition of 262 μM LYD to 3.00 mL LFA solution, and complete mixing, the resulting fluorescence was recorded as I_0 . An addition of 8 – 50 μL of copper(II) sulphate solution (15, 1.5 or 0.15 mM) was then made and the fluorescence signal recorded as I . Similar additions of copper(II) solution were made to LFA in the absence of the LYD and gave fluorescence signals, I_{LFACU} .

Prior to calculations of free and LFA-bound Cu^{2+} , the fluorescence signals were corrected for any dilutions made and then adjusted in the following manner to account for the LFA fluorescence (Equations 3.3 and 3.4).

$$I_0' = I_0 - I_{LFA} \quad (3.3)$$

$$I' = I - I_{LFACU} \quad (3.4)$$

**Table 3-3. LFA and Cu²⁺ Solution Concentrations
for Apparent Chelation Equilibrium Study**

[LFA] mg/L	[Cu ²⁺] μM	[LFA] mg/L	[Cu ²⁺] μM
50	37.2	12.5	14.8
	54.3	6.0	3.96
	61.8		7.91
	78.8	2.0	1.48
25	14.8		1.96
	19.6		2.92
	29.2		3.87
	38.7	0.5	0.50
12.5	4.95		0.99
	9.87		1.96

The inner filter effect resulting from absorbance of the LYD fluorescence by LFA was found to be insignificant and was disregarded. The ratio I_0/I' was then used to determine the concentrations of free and LFA-bound Cu²⁺ by means of the LYD calibration curves generated in Chapter Two.

The data were plotted as the average chelation equilibrium constant for copper binding to LFA, \bar{K} versus the total concentration of fulvic acid in the solution. The number of available metal-ion binding sites on the fulvic acid were calculated based on the approximation 2.9 meq sites/g LFA (31, 32) and the results were replotted as \bar{K} versus percentage coverage of the available binding sites.

3-2.6 Fast Kinetic Uptake of Copper(II) by Humic Acid

The fluorimeter PMT signal was set to zero relative to deionised water. A 20 μL aliquot of 262 μM LYD was added to 3.00 mL of deionised water and mixed well, and the resulting fluorescent signal, I was recorded. The dye was then quenching by a 20 μL – 200 μL addition of Cu^{2+} solution (0.015 – 1.5 mM) and the fluorescence monitored to obtain a constant signal. At $t = 50$ seconds, a 20 μL addition of 400 mg/L LHA solution was made and the fluorescence intensity increased as Cu^{2+} was bound by the humic acid. The fluorescence, I_t was monitored as a function of time and total solution concentrations for a representative sample were 1.72 μM LYD, 0.99 μM Cu^{2+} and 2.6 mg/L LHA.

Using the LYD calibration (Chapter One) and the I_0/I_t experimental ratio, the fluorescence signal was converted into the concentration of copper(II) bound to humic acid, $[\text{Cu-HA}]$, where $[\text{Cu-HA}] = [\text{Cu}]_T - [\text{Cu}]_{\text{free}}$. This concentration was then plotted against time, relative to the point of LHA addition. In order to investigate the kinetics of the copper binding, the data were replotted as $\ln([\text{CuHA}]_f - [\text{CuHA}]_t)$ versus time,

where the subscripts t and f represent the amount of copper bound to humic acid at time, t and the apparent limiting concentration respectively. A Laplace transform analysis (9, 10) was also performed on the CuHA concentration data and $H(k)$, the difference between first and second derivatives was plotted against $\ln(t)$.

3-2.7 Long Term Study of Copper and Humic Acid Interactions

Slow Kinetic Uptake of Copper(II) by Humic Acid

The uptake of copper(II) by humic acid was monitored over an 11 day period of time, in order to study the slow component of binding. An 8.8 mg/L solution of humic acid was adjusted to pH 8.25 and equilibrated for over 24 hours in the dark. 3 mL aliquots of the solution were then transferred to each of six separate 5 mL Nalgene tubes. Aliquots of LYD, and Phenol Red (PR) and Bromocresol Purple (BP) pH indicator dyes, were also added to the tubes as per Table 3-4.

At time zero, 20 μ L 30 mM CuSO_4 (aq) was added to samples 2, 3, 4 and 6. The solutions were well mixed and placed on a rotating stirrer in the dark when not being measured. Beginning at time zero, the fluorescent signal of Samples 1, 2, 5 and 6 were recorded. This measurement was repeated approximately every 24 hours over a period of 11 days. Similarly, absorbance measurements were taken for samples 1 - 4 over the same time period.

Table 3-4. Sample Composition for Long Term Kinetic Uptake of Copper by Humic Acid

Sample No.	V(HA) 8.8 mg/L (mL)	V(Cu ²⁺) 30 mM (μ L)	V(PR) 0.04 wt% (μ L)	V(BP) 0.04 wt% (μ L)	V(LYD) 0.26 mM (μ L)	Signal
1	3.00					$A_1 F_1$
2	3.00	20				$A_2 F_2$
3	3.00	20	50			A_3
4	3.00	20		50		A_4
5	3.00				20	F_5
6	3.00	20			20	F_6

Sample 3 and 4 were used to determine the pH of the solution at the time of measurement. The absorbance signals of the dye alone were equivalent to $A_3 - A_2$ and $A_4 - A_2$. The pH was then calculated as described previously in Section 3-2.2.

The pH for samples 5 and 6 were assumed to vary in the same manner as samples 3 and 4 and based on this information, the value of the LYD-Cu stability constant for static quenching, K_S was determined. The ratio of fluorescent intensities I_0/I corresponded to $(F_5 - F_1)/(F_6 - F_2)$. Calibration curves for copper and humic acid from Chapter Two were employed to ascertain the concentration of free copper(II) in solution. The kinetic

uptake curve was then plotted as the concentrations of copper(II) bound to LHA, $[CuHA]$ against time.

Displacement of Copper(II) from Humic Acid

A long term study of the displacement of bound copper(II) from the humic acid was conducted. From the same equilibrated solution of 8.8 mg/L LHA at pH 8.25, aliquots of the solution (3.00 mL) were transferred to each of sixteen 5mL Nalgene sample tubes. LYD fluorescent dye, Phenol Red (PR), Bromocresol Purple (BP) and Bromocresol Green (BG) pH indicator dyes were then added as per Table 3-5.

At time zero, 20 μ L 30 mM $CuSO_4$ (aq) was added to samples 3, 4 and 11 – 16. The solutions were well mixed and placed on a rotating stirrer in the dark. After the addition of copper, the pH of the solutions (except sample 3) was rapidly decreased to cause the displacement of bound copper from humic acid. This was achieved by additions of 2.5 mM sulfuric acid (90, 120 or 200 μ L) and resulted in final solution pH values of 6.5, 5.5 and 3.3. Fluorescence and absorbance of the solutions was then recorded to monitor the displacement of copper from the humic acid.

Two further sets of solutions were prepared having compositions identical to samples 11-16. For these solution sets, copper and humic acid were allowed a longer equilibration time prior to the addition of acid. Acidification was conducted after 1 and 5 days (for the first and second sets respectively), relative to the time that copper was added to the LHA.

**Table 3-5. Sample Composition for Long Term Kinetic Displacement
of Copper by Humic Acid**

Sample No.	V(HA) 8.8 mg/L (mL)	V(Cu²⁺) 30 mM (μL)	V(H₂SO₄) 2.5 mM (μL)	V(pH dye) 0.04 wt% (μL)	V(LYD) 0.26 mM (μL)	Signal
1	3.00		90			<i>A₁ F₁</i>
2	3.00		200			<i>A₂ F₂</i>
3	3.00	20				<i>A₃ F₃</i>
4	3.00	20	200			<i>A₄ F₄</i>
5	3.00		90	50 (<i>BP</i>)		<i>A₅</i>
6	3.00		120	50 (<i>BP</i>)		<i>A₆</i>
7	3.00		200	50 (<i>BG</i>)		<i>A₇</i>
8	3.00		90		20	<i>F₈</i>
9	3.00		120		20	<i>F₉</i>
10	3.00		200		20	<i>F₁₀</i>
11	3.00	20	90	50 (<i>BP</i>)		<i>A₁₁</i>
12	3.00	20	120	50 (<i>BP</i>)		<i>A₁₂</i>
13	3.00	20	200	50 (<i>BG</i>)		<i>A₁₃</i>
14	3.00	20	90		20	<i>F₁₄</i>
15	3.00	20	120		20	<i>F₁₅</i>
16	3.00	20	200		20	<i>F₁₆</i>

Data Processing

For each non-quenched LYD fluorescent signal, $I_0(t)$ (samples 8 – 10), the solution pH was followed by monitoring the absorbance, $A_0(t)$ of the corresponding pH indicator dye solutions (samples 5 – 7). Corrections to the signals were made to account for absorbance and fluorescence of the humic acid (samples 1, 2). An example of these adjustments for a 200 μL addition of acid would be $A_0'(t) = A_7 - A_2$ for absorbance and $I_0'(t) = F_{10} - F_2$ for fluorescence.

In the same way, for quenched LYD fluorescent signals, $I(t)$ (samples 14 - 16), the solution pH was followed by monitoring the absorbance, $A(t)$ of the corresponding pH indicator dye solutions (samples 11 - 13). In a similar manner, the signals were corrected account for humic acid absorbance and fluorescence (samples 3, 4). For a 200 μL acid addition, $A'(t) = A_{13} - A_4$ and $I'(t) = F_{10} - F_4$.

The value of the stability constant for static quenching of the LYD by Cu^{2+} , K_S was determined from the calculated solution pHs. Calibration curves for copper and humic acid from Chapter Two were employed to ascertain the concentration of free copper(II) in solution. The kinetic displacement curve was then plotted as the concentrations of copper(II) bound to LHA, $[\text{CuHA}]$ against time, relative to the time of acid addition to the samples.

3-3 Results and Discussion

3-3.1 Uptake Kinetics of Copper(II) by LFA

Previous studies of the metal release rates from fulvic acid have revealed a number of kinetic components. Lavigne, Langford and Mak (12) found four kinetic species of Ni^{2+} with rate constants ranging from 0.67 to 0.0026 s^{-1} when they investigated the release of nickel(II) from Armadale fulvic acid. In their study, the formation of the detectable complex NiPAR was monitored by absorbance. Few studies of metal uptake kinetics by humic substances have been performed in the past, due to detection difficulties, and it was predicted that the current investigation into the binding rate of copper(II) by the LFA, would reveal a number of kinetic components.

It was found that when LFA was added to a well mixed solution of LYD and copper(II), the fluorescence signal increased significantly, owing to the removal of free Cu^{2+} from solution by fulvic acid binding. Thus the overall quenching of LYD was reduced. Figure 3-1 depicts the LYD fluorescence monitored as a function of time for a representative sample, where addition of the fulvic acid solution gave total concentrations of $1.52 \mu\text{M}$ LYD, $1.64 \mu\text{M}$ $\text{Cu}^{2+}(\text{aq})$ and 44 mg/L LFA.

It was clear from the vertical jump in the fluorescence signal to a stable value upon the addition of the LFA, that the kinetics of uptake were too fast to be analyzed by this

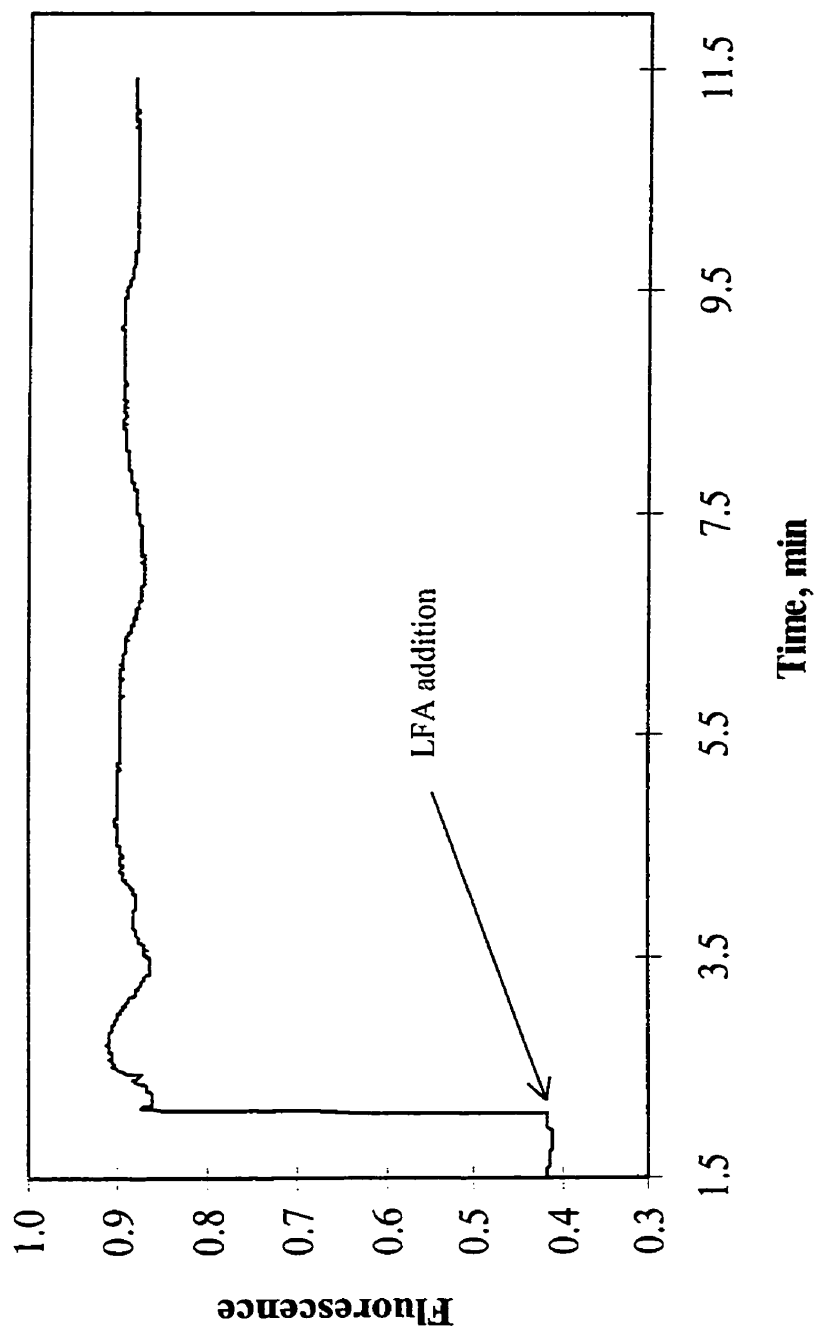


Figure 3-1. Kinetic uptake of copper(II) by fulvic acid. Fluorescence monitored as a function of time showing 2.15 μM LYD (pH 5.6, 10 ± 2 °C) initially quenched by 2.31 μM Cu^{2+} . Addition of fulvic acid solution (1mL, $t = 2.10$ min) gave total concentrations of 1.52 μM LYD, 1.64 μM Cu^{2+} (aq) and 44 mg/L LFA. Copper(II) was rapidly bound by LFA.

particular LYD quenching technique. Nevertheless, useful information was provided about the system. The result confirmed that the equilibrium between Cu^{2+} and LYD was labile, as Cu^{2+} release from the LYD was too rapid to be seen on the measurement timescale. As the water exchange rate of the hexaaquacopper ion, $\text{Cu}(\text{OH}_2)_6^{2+}$ was known to be extremely rapid ($10^{8.4} \text{ s}^{-1}$) (33) and at least four orders of magnitude larger than for $\text{Ni}(\text{OH}_2)_6^{2+}$, the result was not altogether surprising.

The rapid uptake of copper also indicated that the LFA metal-ion binding sites must have been relatively accessible to the Cu^{2+} . However, it should be noted that calculations based on 2.9 meq sites/g LFA (31, 32) indicated that only 0.8% of the available binding sites were occupied by Cu^{2+} . It is possible that significantly higher ratios of copper to fulvic acid may have been required in order to observe the slower binding components.

3-3.2 Apparent Chelation Equilibrium of Copper(II) with LFA

The chelation equilibrium of copper(II) binding to fulvic acid has been studied in detail by Gamble, Underdown and Langford (34). The authors monitored copper(II) with an ion selective electrode and also recorded the absorbance of fulvic acid. A clear trend in chelation equilibrium constants with varying metal to fulvic acid ratios was observed. In the study, concentration ratios varied from 0.100 – 6.000 mmol Cu(II) per gram fulvic acid, and the authors reported the largest equilibrium constants for the lowest metal to FA ratios, where only the stronger binding sites were occupied. The equilibrium constant

decreased by an order of magnitude between binding ratios of 0.100 to 0.400 mmol Cu(II)/g FA and then by a further factor of four between ratios of 0.400 to 1.000 mmol Cu(II)/g FA. For all higher binding ratios, little variation in the measured value of the equilibrium constant was observed.

A similar study was performed for this thesis using the indirect fluorescent probe technique of analysis, with 20 solutions of varied copper(II) and fulvic acid concentrations. Following the establishment of apparent equilibrium in each of the solutions, the fluorescence quenching was measured and the concentration of free and bound Cu^{2+} calculated. For apparent equilibrium calculations, an average binding site, LFA_x was assumed (Equation 3.5) and \bar{K} was then determined via Equation 3.6 below.



$$\bar{K} = \frac{[CuLFA_x]}{[LFA_x][Cu^{2+}]} \quad (3.6)$$

Values of \bar{K} were calculated for $[CuLFA_x]$ and $[Cu^{2+}]$ in molar concentration units and $[LFA_x]$ in units of mg/L, and the results are depicted in Figure 3-2, plotted against the total concentration of fulvic acid, $[LFA]$. Linear regression analysis of the data gave a correlation coefficient of $R^2 = 0.021$ indicating the significant spread of the data. No clear trend was observed and \bar{K} was estimated as 2.7 ± 0.8 L/mg.

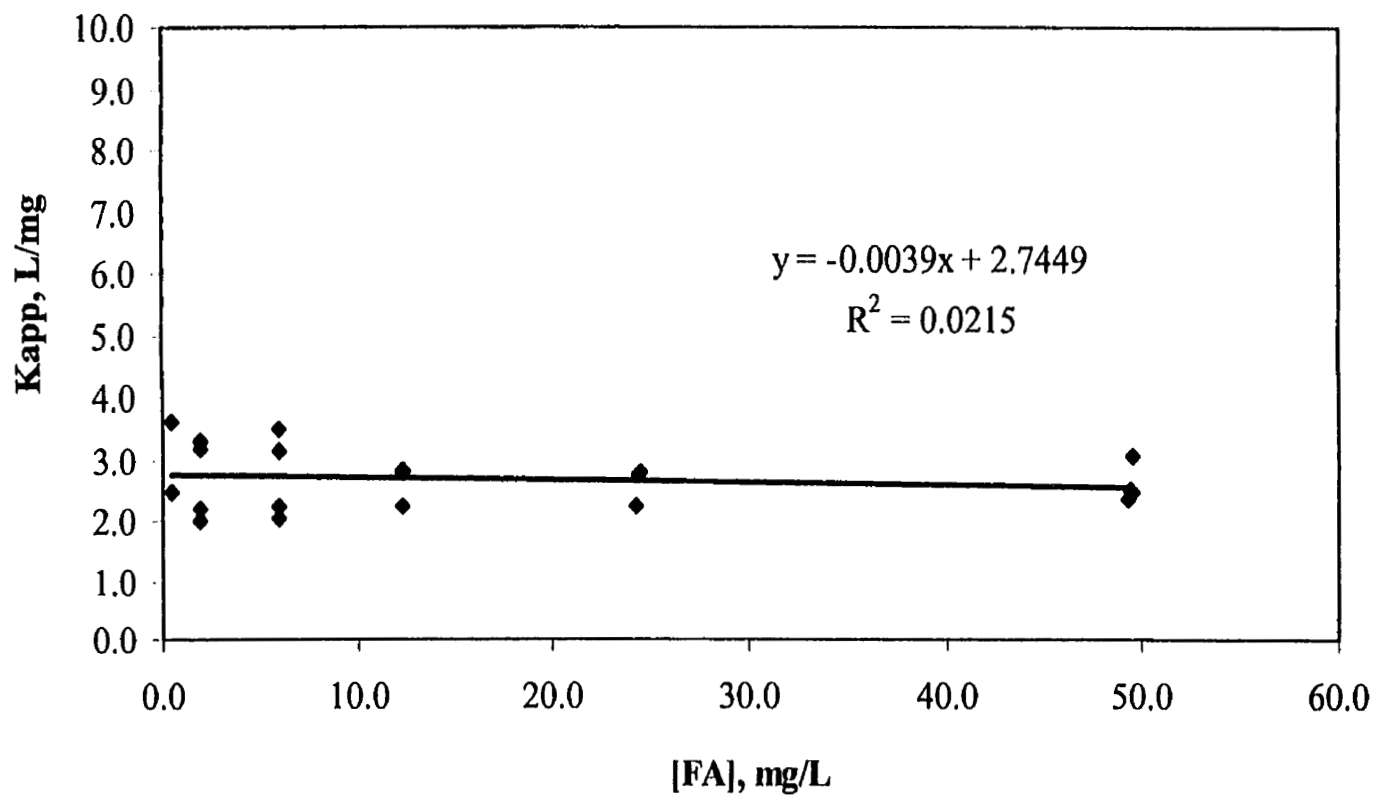


Figure 3-2. A plot of the apparent chelation equilibrium constant $K = [FA-Cu]/[FA].[Cu^{2+}]$ against the total concentration of fulvic acid. $[FA-Cu]$ and $[Cu^{2+}]$ represent the molar concentrations of bound and free copper(II) respectively and $[FA]$ is the total concentration of fulvic acid in mg/L. A quadratic trendline was fit to the data and the equation of the line and correlation coefficient are shown.

It has been reported in the literature that fulvic acid possesses an average of 2.9 meq metal ion binding sites per gram (31, 32). This figure was employed to calculate the total number of available binding sites on the LFA and determine the percentage site coverage for every experimental Cu^{2+} : LFA ratio. The data were replotted as \bar{K} (L/mol) against the percentage site coverage and the results are shown in Figure 3-3.

Comparison with Previous Study

It can be seen that the approximate range of LFA site coverage in this experiment was 10 – 50 % and no clear trend of decreasing average equilibrium values could be established. This corresponded to a concentration range of 0.39 to 1.00 mmol Cu(II) per gram LFA, over which range Gamble, Underdown and Langford had measured a fourfold decrease in equilibrium constant values. Further investigation is required to understand this discrepancy. It may be possible that a proportion of the copper was trapped in the electrical double layer around the LFA polyelectrolyte and was diffusionally restricted from interacting with the LYD. The data in Figure 3-3 pointed to an average \bar{K} of $1.3 \times 10^6 \pm 0.3 \times 10^6$ L/mg.

Experimental concentration ratios of Cu(II) to LFA had been chosen in order to obtain significant LYD fluorescence signal quenching ($I_t < 0.9 \cdot I_0$). For fulvic acid binding site coverage less than 10%, the remaining free copper in the solution was not large enough to cause accurately measurable LYD quenching. This constituted a limitation of the technique.

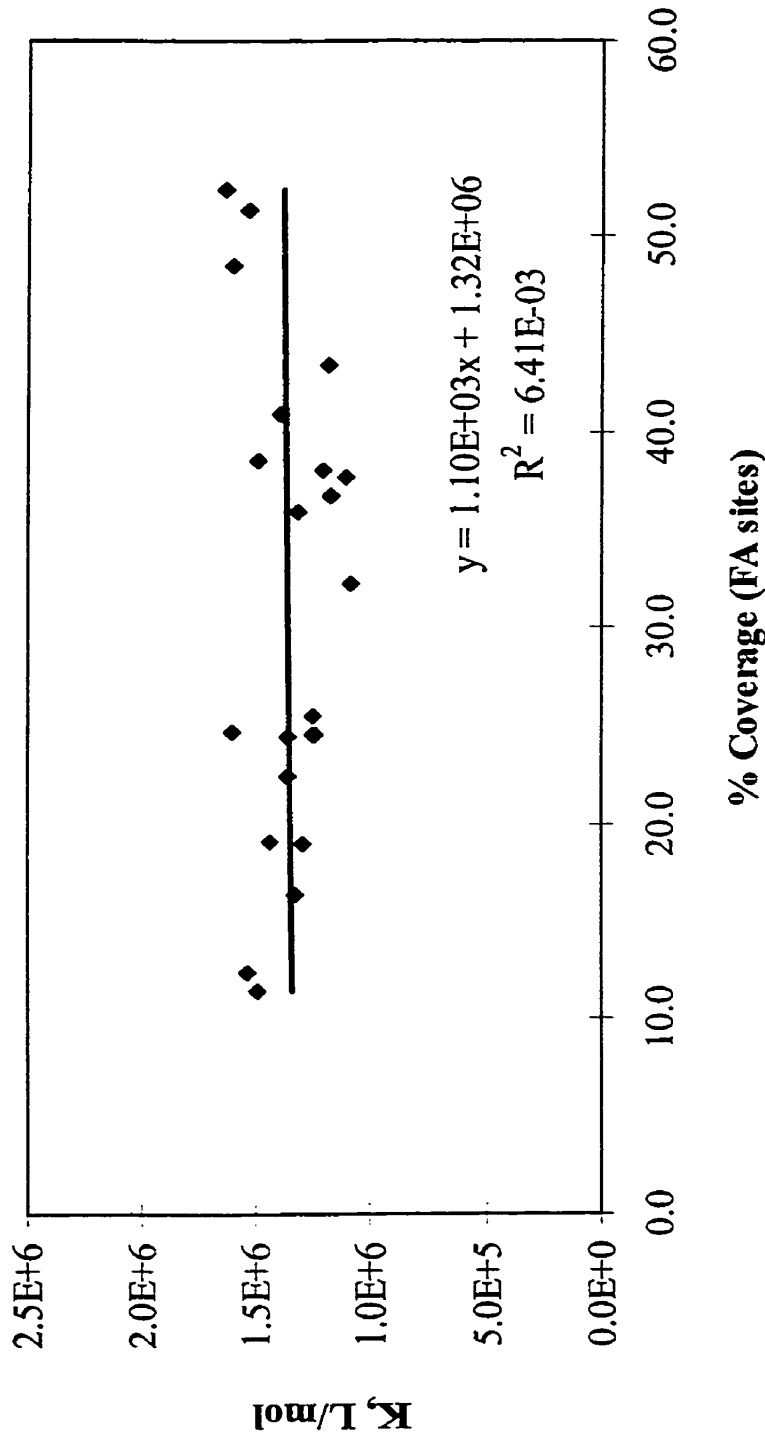


Figure 3-3. A plot of the apparent chelation equilibrium constant $K = [FA-Cu]/[FA].[Cu^{2+}]$ against the percentage coverage of fulvic acid binding sites (assuming 2.9 meq sites/g). $[FA-Cu]$ and $[Cu^{2+}]$ represent the molar concentrations of bound and free copper(II) respectively and $[FA]$ is the total concentration of fulvic acid binding sites. A quadratic trendline was fit to the data and the equation of the line and correlation coefficient are shown.

3-3.3 Rapid Kinetic Uptake of Copper(II) by LHA

Humic versus Fulvic Acid Kinetics

In comparison to fulvic acids, humic acids exist as much larger and more complex polyelectrolytes. As a result, the metal binding sites on LHA were predicted to show wider variation. The uptake kinetics of copper(II) by humic acid at pH 6.0 were investigated using LYD quenching as an indirect probe. The resulting continuous time fluorescence spectrum is shown in Figure 3-4. Following the addition of humic acid to a solution containing LYD and Cu^{2+} , there was a gradual increase of the fluorescence signal toward a limiting value, which indicated a significantly slower rate of copper(II) uptake than was observed for the fulvic acid.

Calculations based on the LYD calibration curves and the relationship $[\text{CuHA}] = [\text{Cu}]_T - [\text{Cu}]_{\text{free}}$ allowed replotting of the data as the concentration of copper bound to humic acid against time, relative to the point of humic acid addition (Figure 3-5). This plot revealed that the majority of the uptake was completed in the first 100 seconds and the curve approached a limiting value of $5.1 \times 10^{-7} \text{ M Cu}^{2+}$ bound ($= [\text{CuHA}]_f$).

Determination of Rate Constants

In order to determine whether the uptake kinetics could obey simple first order kinetics, a plot of $\ln([\text{CuHA}]_f - [\text{CuHA}]_t)$ against time was constructed (Figure 3-6). Although the

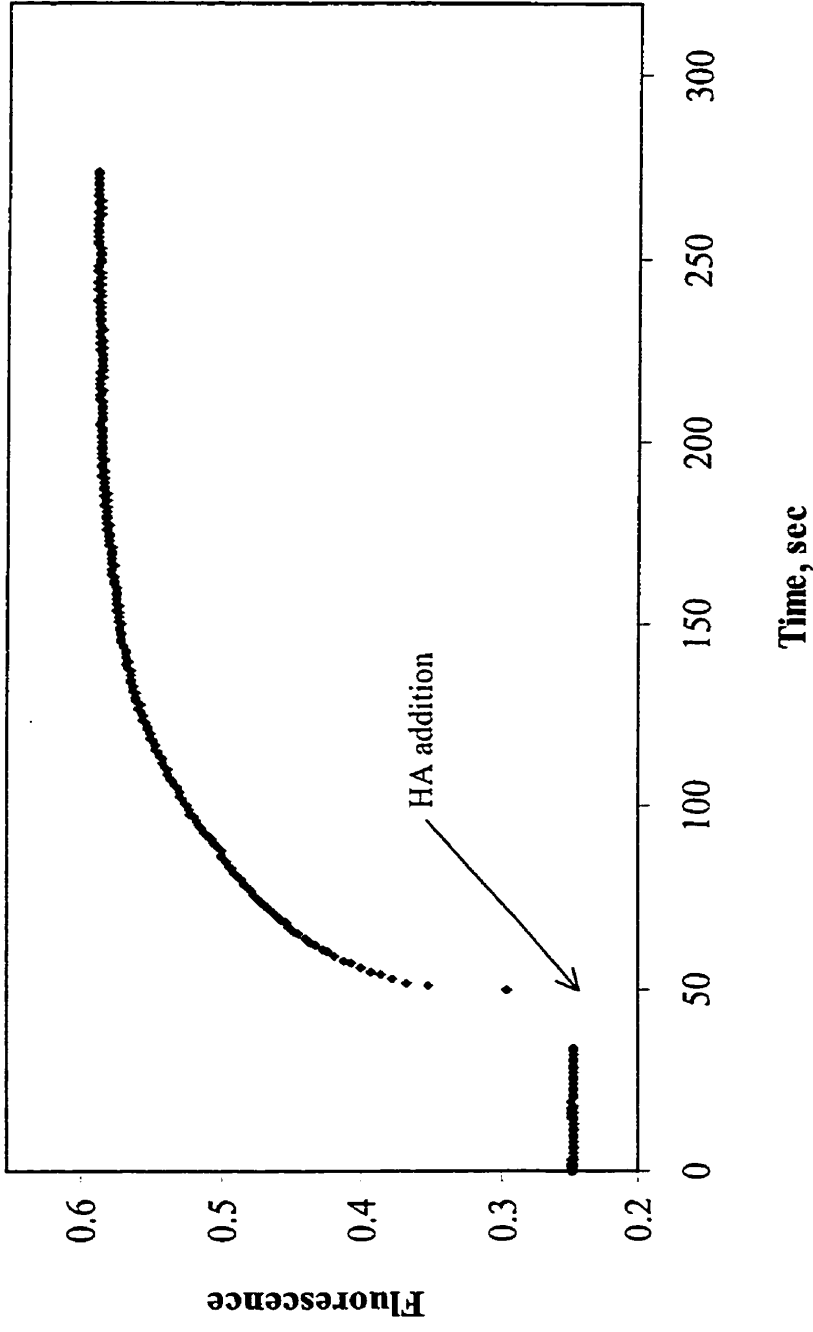


Figure 3-4. Kinetic uptake of copper (II) by humic acid (pH 6.0). Fluorescence monitored as a function of time showing 1.72 μM LYD initially quenched by 0.99 μM Cu^{2+} . Upon addition of humic acid solution (20 μL) at time, $t = 50$ seconds, quenching decreases as copper is bound by humic acid (2.6 mg/L total concentration).

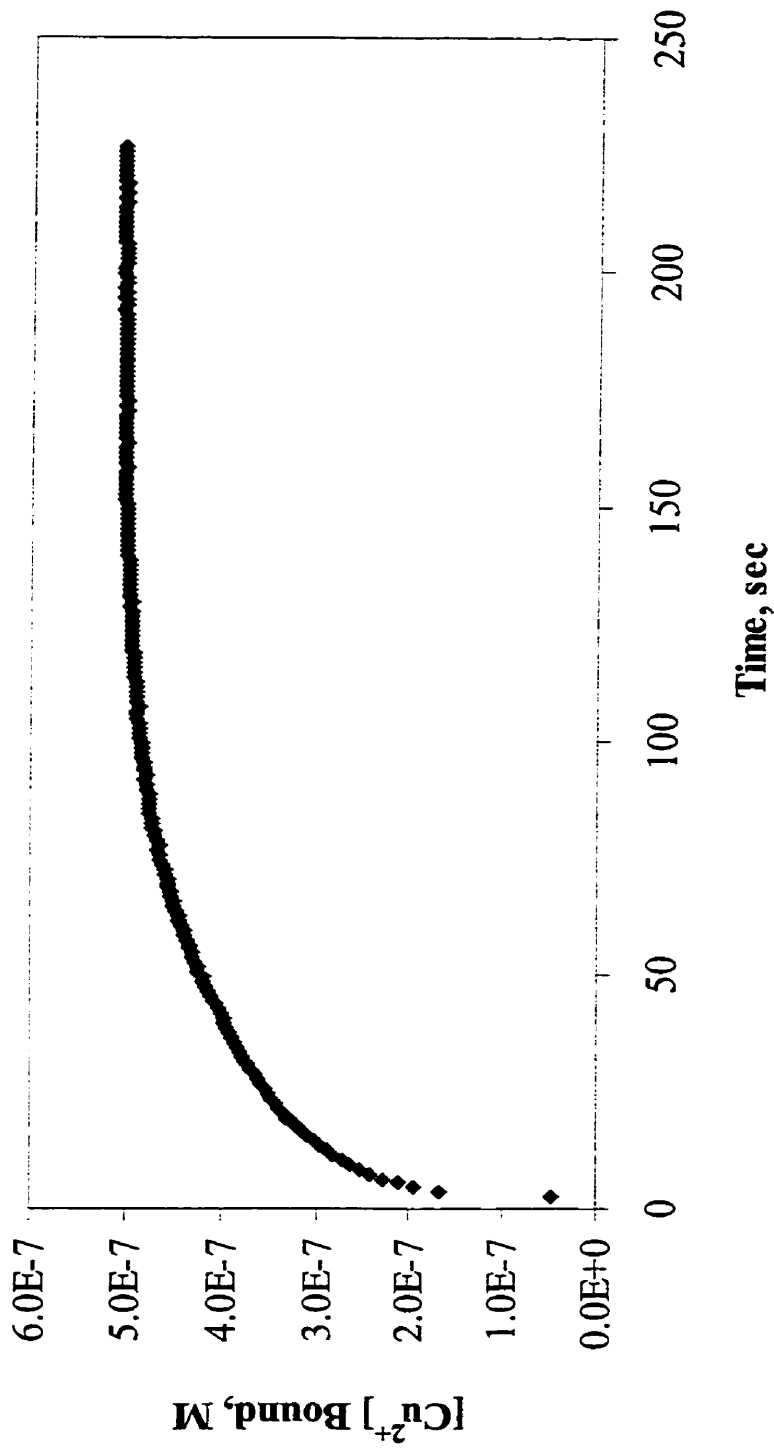


Figure 3-5. Kinetic uptake of copper (II) by humic acid. Concentration of copper bound to humic acid, plotted against time. Time zero represented the addition of HA and the concentration of copper bound was determined from LYD quenching calibration and using $[Cu-HA] = [Cu]_T - [Cu]_{free}$.

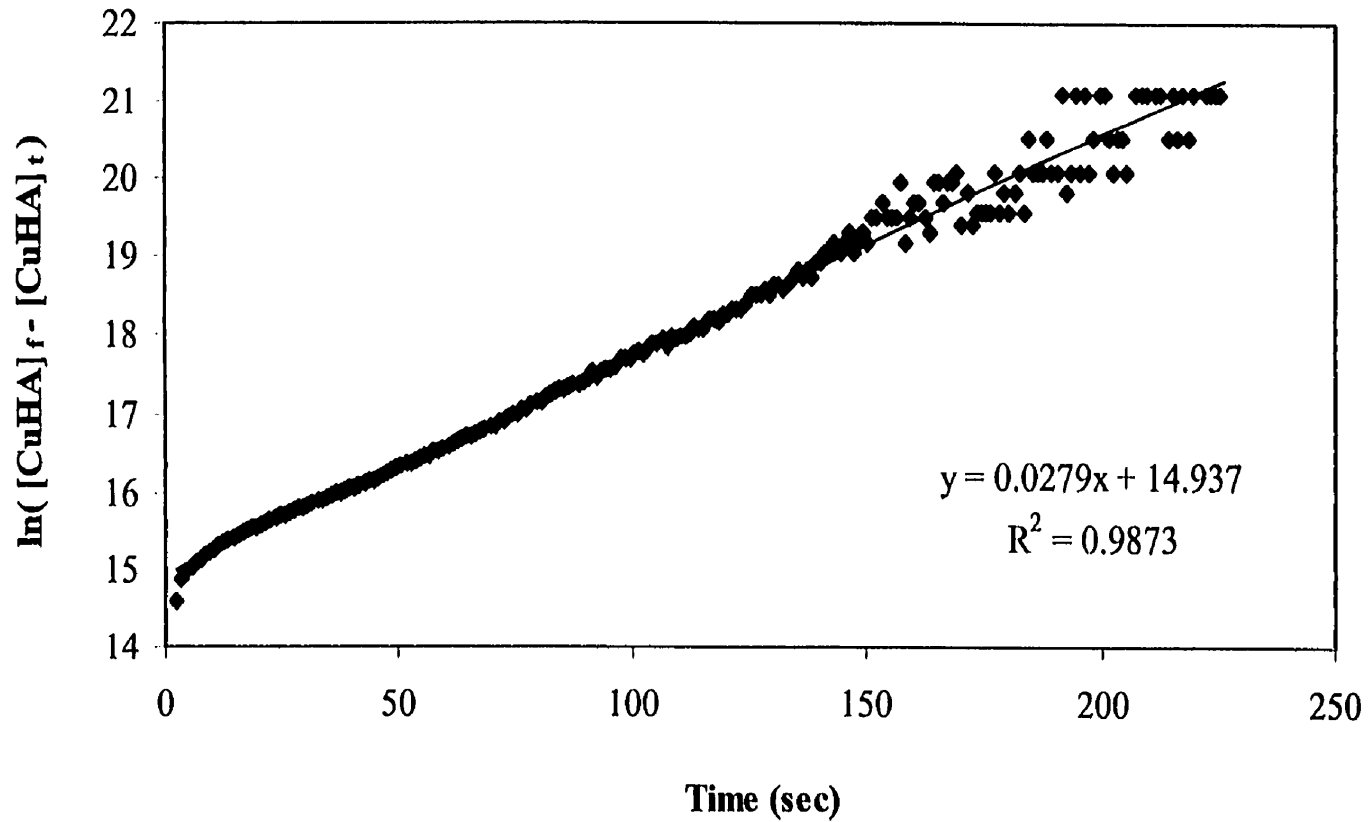


Figure 3-6. *First order kinetics plot for uptake of copper (II) by humic acid.* The concentration of copper bound to humic acid at time, t and the apparent limiting concentration are given as $[CuHA]_t$ and $[CuHA]_f$ respectively. A quadratic trendline was fit to the data and the equation of the line and correlation coefficient are shown.

data shows reasonable correlation ($R^2 = 0.987$) with a straight line fit and indicated an average rate constant of 0.028 s^{-1} , there appeared to be a hint of the existence of a second, faster component in the early region of the plot. The scatter of data observed for times greater than 150 seconds can be attributed to a reduced sensitivity of fluorescence measurement, as the quenching decreased and the difference between I_0 and I became progressively smaller.

The Laplace transform method was used to obtain estimates of the contributing rate constants. Before the analysis could be performed, the $[CuHA]$ data needed to be smoothed by fitting to a polynomial curve. As logarithmic coordinates have been found to optimize the data for polynomial fitting (12), a plot of $\ln[CuHA]$ versus $\ln(t)$ was made. Microsoft Excel least squares polynomial fitting accurately reproduced the data for a 6th degree polynomial, (Equation 3.7) and the polynomial is shown superimposed on the experimental data in Figure 3-7.

$$y = -0.003016x^6 + 0.06209x^5 - 0.5099x^4 + 2.129x^3 - 4.708x^2 + 4.798x + 113.81 \quad (3.7)$$

where x and y represent $\ln(t)$ and $\ln[CuHA]$ respectively.

The first and second derivatives of the smoothed $[CuHA]$ data were found with respect to $\ln(t)$ and the function $H(k)$ was plotted against $\ln(t)$ (Figure 3-8). The Laplace transform plot represented the distribution of rate constants, k about peak values and two peaks were evident with corresponding values of $\ln(t)$. The values were related to $k (=2/t)$ and

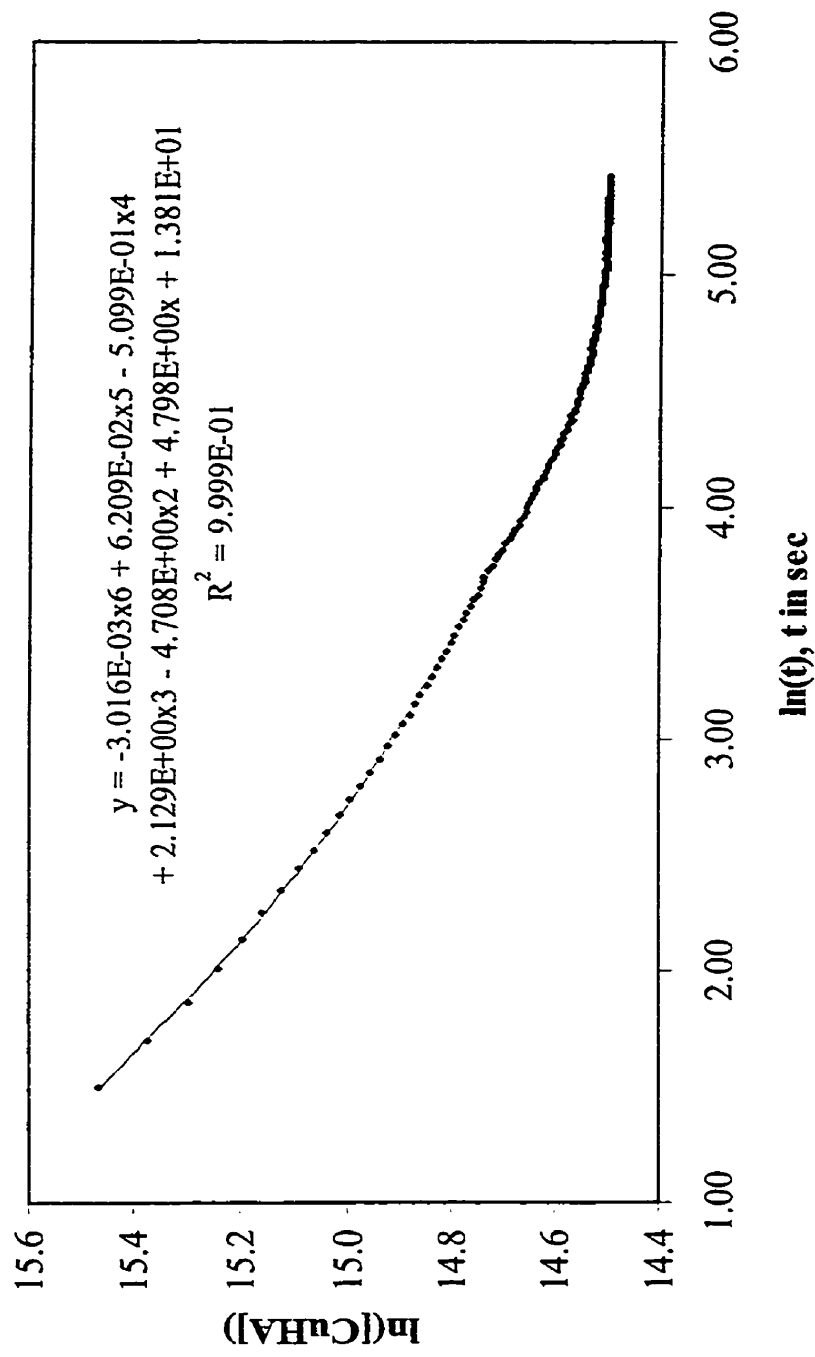


Figure 3-7. *Data smoothing for Laplace transform analysis of kinetic data.* The kinetic uptake data for copper(II) by HA was plotted as the natural logarithms of [CuHA] and time. The closest polynomial fit for the data was then determined via Microsoft Excel and the resulting 6th order polynomial curve (and equation) is shown superimposed on the experimental data.

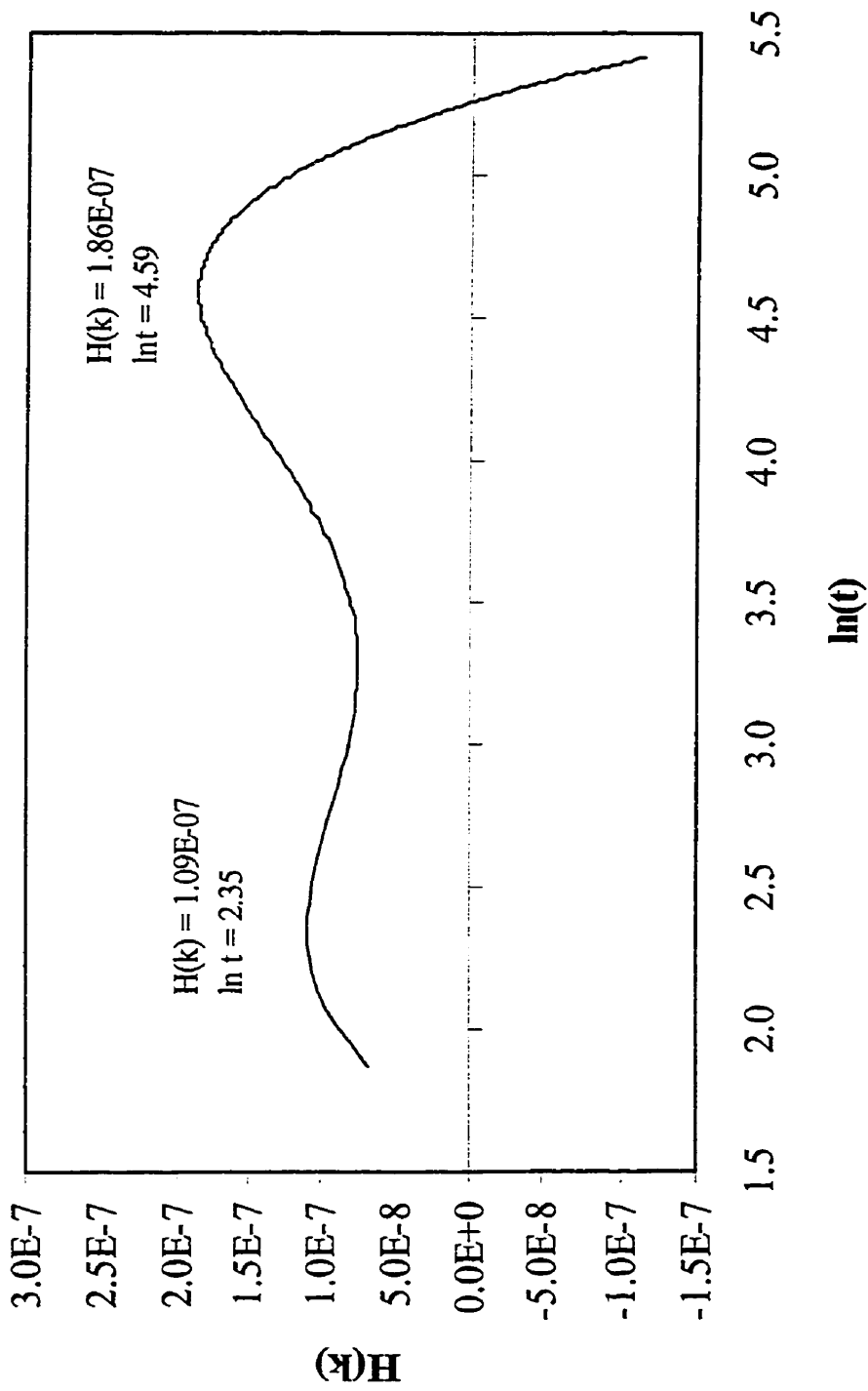


Figure 3-8. Laplace transform analysis of kinetic data. $H(k)$ represents the difference between first and second derivatives of the [CuHA] concentration data with respect to $\ln t$. The variable k is equal to $2/t$.

the two main component rate constants for the uptake of copper by LHA were calculated to be 0.19 sec^{-1} and 0.020 sec^{-1} . As the area of the peak is proportional to the concentration of the component (9,10,14), it can be clearly seen that there was a majority of the slower binding species at this pH and ligand to metal ratio.

Comparison to Previous Stripping Studies

In studying the stripping kinetics of copper(II) from humic acid, Bonifazi, Pant and Langford had found that 84% of the copper reacted within the 1.5 second mixing time of the experiment and was judged to come from highly labile CuHA complexes. Middle and slow kinetic components had also been identified by the authors, having rate constants of $0.093 \pm 0.013 \text{ sec}^{-1}$ and $0.0077 \pm 0.0008 \text{ sec}^{-1}$ respectively. Assuming that the complexing sites for copper on the humic acid are ordinary chelating sites, the metal-ion uptake would be expected to occur more rapidly than the release. Following chelation of copper with one donor ligand on the humic acid, the proximity of the second donor ligand and the labilisation of the remaining waters of hydration on the Cu^{2+} would increase the binding rate. The above result appears to confirm this assumption, as the measurable component uptake rates were significantly faster (0.19 sec^{-1} and 0.020 sec^{-1}) than for the stripping experiment.

Validity of Experimental Rate Constants

However, due caution needs to be observed in the interpretation of results, as the second-order Laplace transform approximation is sensitive to artifacts and may introduce peak

broadening (14). In order to be confident that the values obtained represent rate constants and are not simply a mathematical byproduct, Langford and Gutzman have proposed two key tests.

1. With varying pH and concentration ratios of LHA/Cu²⁺, the rate constants should remain stable, although the relative proportion of the components will change.
2. These changes in component concentrations should follow mass action principles.

Therefore further tests at a range of pH values and concentration ratios need to be performed, to confirm the validity of the kinetic components found for the uptake of copper by LHA. It should also be noted that the identification of a discrete number of component rate constants, would not imply that these refer to specific molecular species (14). However, the establishment of kinetic components for a system would permit the rate constants to be grouped into distinctive sets, based on these components. Within these sets, it would still be possible for the individual sites to show considerable diversity (14).

An additional test involves using the rate components found via the Laplace transform analysis as input parameters to a non-linear regression (NLR) analysis of Equation 1.1

(Chapter 1). For meaningful Laplace transform results, the regressions should converge and the output parameters should be related sensibly to the input parameters (14). When an NLR analysis (Table Curve Software) was performed on the CuHA kinetic uptake data, convergence was achieved. However, the limited number of input parameters resulted in a fitted curve that did not accurately represent the data.

3-3.4 Slow Kinetic Uptake of Copper(II) by LHA

The uptake of copper by humic acid was monitored over an 11 day period to study their long term interaction. Figure 3-9 shows the concentration of copper(II) bound by humic acid, relative to the time of copper addition. It was evident that a much slower kinetic uptake component existed, as the $[CuHA]$ increased over the first 3 days, then approached a limiting value. However, owing to the limited number of data points and approximate nature of the trendline, it was not possible to estimate a slow rate constant for the uptake process with any accuracy.

3-3.5 Displacement of Copper(II) from LHA

As humic acid exists in solution as a complex mixture of polyelectrolytes, with conformation dependent on pH and ionic strength, the binding of metal ions will be more complicated than for the smaller fulvic acids. It has been proposed that there may be

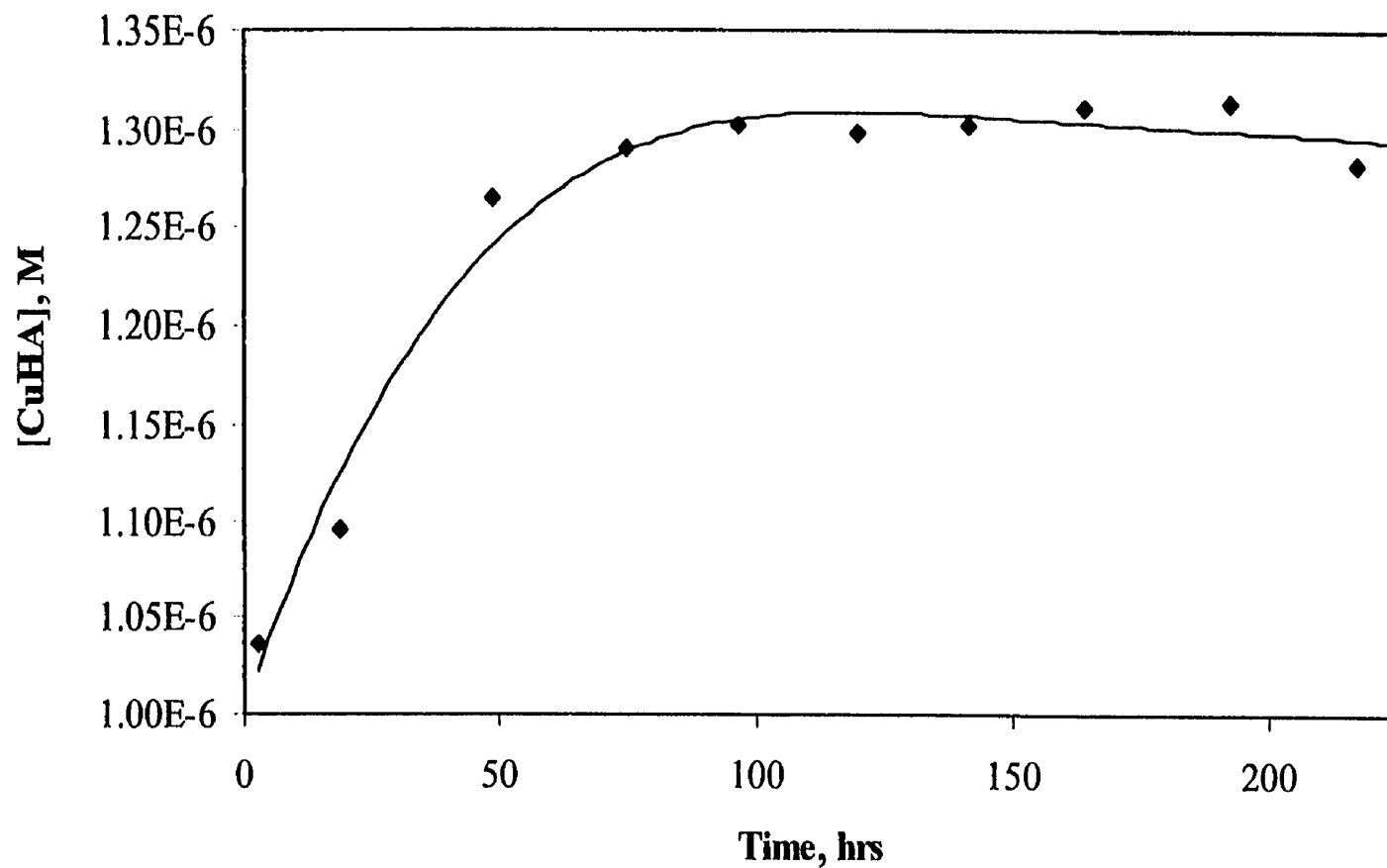


Figure 3-9. *Slow kinetic uptake of Cu^{2+} by humic acid.* The concentration of copper bound by humic acid, [CuHA] is plotted relative to time of copper addition.

slow diffusion of metal ions to the inside of the LHA colloids to stronger binding sites (11). When the pH is reduced, H^+ ions displace the Cu^{2+} which is then released into solution and can be detected by quenching of the LYD fluorescence.

A study was performed over a period of 11 days where an equilibrated LHA and copper(II) solution at pH 8.25 was acidified (to pH 6.5, 5.5, 3.3) at time 0, 1 and 5 days, relative to the time of copper addition. For each of the acidified solutions, the concentration of bound copper(II) was monitored over at least a five day period. The resulting Cu^{2+} displacement from the humic acid is represented as a plot of bound $[CuHA]$ versus time, relative to the time of acidification in Figure 3-10.

The results are largely inconclusive. It was expected that a sample containing LHA and copper that had been equilibrated for 5 days at pH 8.25 prior to acidification would show a slower rate of Cu^{2+} release, as the copper had had a longer time to diffuse to any less accessible HA binding sites. It was also predicted that acidification to pH 3.3 would initiate the displacement of significantly more copper from LHA than for the higher pH values of acidification. This distinction was also not seen. The scatter of the data severely limited the experimental interpretation. The result did seem to imply that little copper was released from the LHA over this timeframe, and that similar binding sites were occupied after 0 and 5 days, however further investigation would be required to fully interpret this result.

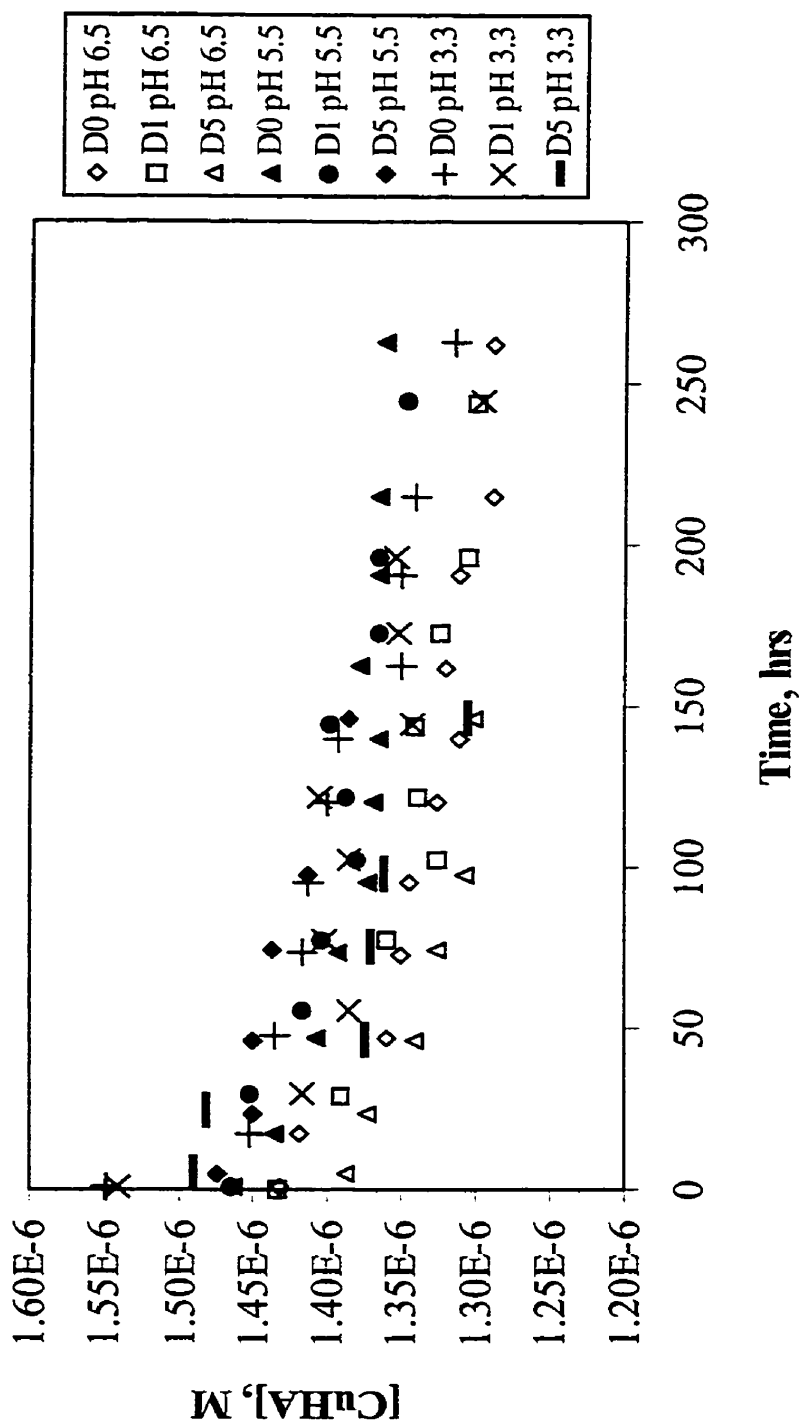


Figure 3-10. Release of Cu^{2+} from humic acid. Copper and HA were equilibrated at pH 8.25 for a period of time ($D0=0$ days, $D1=1$ day, $D5=5$ days) to allow slow binding of copper to HA. Following this time, acid was added to reduce the pH of the solution (to pH 6.5, 5.5 or 3.3) and the release of Cu^{2+} from the HA was monitored. $[CuHA]$ was plotted against time, relative to the time of acid addition.

3-4 Summary

The calibration of Lucifer Yellow fluorescent dye quenching by Cu^{2+} , as determined in Chapter Two, was used as a tool for the investigation of copper(II) speciation with fulvic and humic acids. The rapid uptake of Cu^{2+} by LFA occurred too quickly to be measured by the above technique. However, the result confirmed that the equilibrium between Cu^{2+} and LYD was labile, and indicated that the LFA metal-ion binding sites must have been relatively accessible to the Cu^{2+} .

In studying the equilibrium behavior of copper(II) with LFA, no apparent trend was observed and \bar{K} was estimated as 2.7 ± 0.8 L/mg. Based on 2.9 meq metal ion binding sites per gram LFA, the experimental range of site coverage was 10 – 50% which pointed to an average \bar{K} of $1.3 \times 10^6 \pm 0.3 \times 10^6$ M^{-1} . The analysis technique showed a detection limit of 10^{-7} M Cu^{2+} , which prevented the study of smaller percentage site coverages.

The fast uptake kinetics of copper(II) by humic acid at pH 6.0 were investigated. A first order plot of the concentration data, as $\ln([\text{CuHA}]_f - [\text{CuHA}]_t)$ against time, gave a predominantly straight line fit and indicated an average rate constant of 0.028 s^{-1} . When a Laplace transform analysis was performed, two component rate constants were found (0.19 sec^{-1} and 0.020 sec^{-1}) and the slower component appeared to be present in greater proportion. However, further experiments at a variety of ligand to metal ratios and pH values are required, to confirm the validity of the kinetic components.

A further, slow component of copper uptake by humic acid was found in a long term study. The $[CuHA]$ was found to increase over a period of 3 days, then approached a limit. The spread of the data did not allow a rate constant to be determined. Finally, in a study of long term displacement kinetics of Cu^{2+} from LHA, the results were largely inconclusive and implied that there was insignificant difference in the rate or amount of copper displaced from LHA, as pre-acidification equilibration time and displacement pH were varied. This result requires further investigation to be properly interpreted.

CHAPTER 4

CONCLUSION AND SUGGESTIONS FOR FURTHER RESEARCH

4-1. Conclusion

Metal speciation studies with natural ligands have been widely studied in the past, however many of the methods of analysis have either suffered from a severe lack of sensitivity, or produced ambiguous results. This thesis focussed on the investigation of a fluorescent probe technique for the analysis of free metal ion concentrations, and its suitability for kinetic speciation applications. The chosen probe, Lucifer Yellow fluorescent dye (LYD) was selective for quenching by free copper(II) ions and was used as a means to study the kinetic and equilibrium speciation of Cu^{2+} with Laurentian fulvic (LFA) and humic acids (LHA). Chapter One described the characterization of the fluorescent dye and generation of a predictable calibration curve. Applications of the fluorescence quenching method were outlined in Chapter Two. The key findings of this work are detailed below.

- (1) The quenching behaviour of the LYD with respect to copper(II) generated a non-linear Stern-Volmer relationship. A static quenching mechanism was found to predominate and could be modeled by a linear relationship derived by Castanho and Prieto.

- (2) The relationship of the fluorescence quenching ratio, I_0/I to free Cu^{2+} concentration was highly pH dependent, and the stability constant for static quenching, K_S was found to vary from $\log K_S = 6.24$ at pH 4.1, to $\log K_S = 8.60$ at pH 9.1. In addition, the equilibrium between copper(II) and the LYD was found to be highly labile.
- (3) Kinetic uptake experiments with LFA revealed that the rate of copper binding to fulvic acid was too rapid to be observed on the timescale of measurement, and suggested that the LFA metal-ion binding sites must have been easily accessible to the copper(II).
- (4) The apparent chelation equilibrium constant, \bar{K} for copper(II) binding to LFA at pH 5.60 was found to be 2.7 ± 0.8 L/mg. Using the approximate literature value of 2.9 meq sites per gram of LFA (31, 32), the overall site coverage ranged from 10 – 50%, with $\bar{K} = 1.3 \times 10^6 \pm 0.3 \times 10^6 \text{ M}^{-1}$.
- (5) Uptake kinetics of copper(II) by LHA were investigated over short (10 min) and long (11 days) timeframes. When analysed by the Laplace transform method, the fast uptake experiment at pH 6.0 suggested the presence of two kinetic components, having rate constants of 0.19 sec^{-1}

and 0.020 sec^{-1} , with the slower component in higher proportion. However, the reliability of the components would need to be confirmed by repeating the experiment over a range of pH and ionic strength conditions.

- (6) An additional, much slower component was found at pH 8.2 during the 11 day uptake experiment, where the concentration of copper bound to LHA was seen to increase over three days before approaching a limit.
- (7) Little difference in the displacement kinetics of copper from LHA (upon acidification) was evident, for changing equilibration times and final pH. There were variations of zero to five days in the Cu^{2+} /LHA equilibration time prior to acid addition, and resulting acidification pH values of 6.5, 5.5 and 3.3.

4-2. Suggestions for Further Research

Preliminary studies reported in this thesis employed a fluorescent probe for the detection of free metal ions in solution, and the results indicated that this was a promising technique for some kinetic speciation applications, giving reasonably high sensitivity. It would be interesting to investigate the use of a range of anionic fluorescent dyes that are selectively quenched by particular contaminant metal ions. However, before this

approach can be applied to natural water samples, many additional laboratory tests are required.

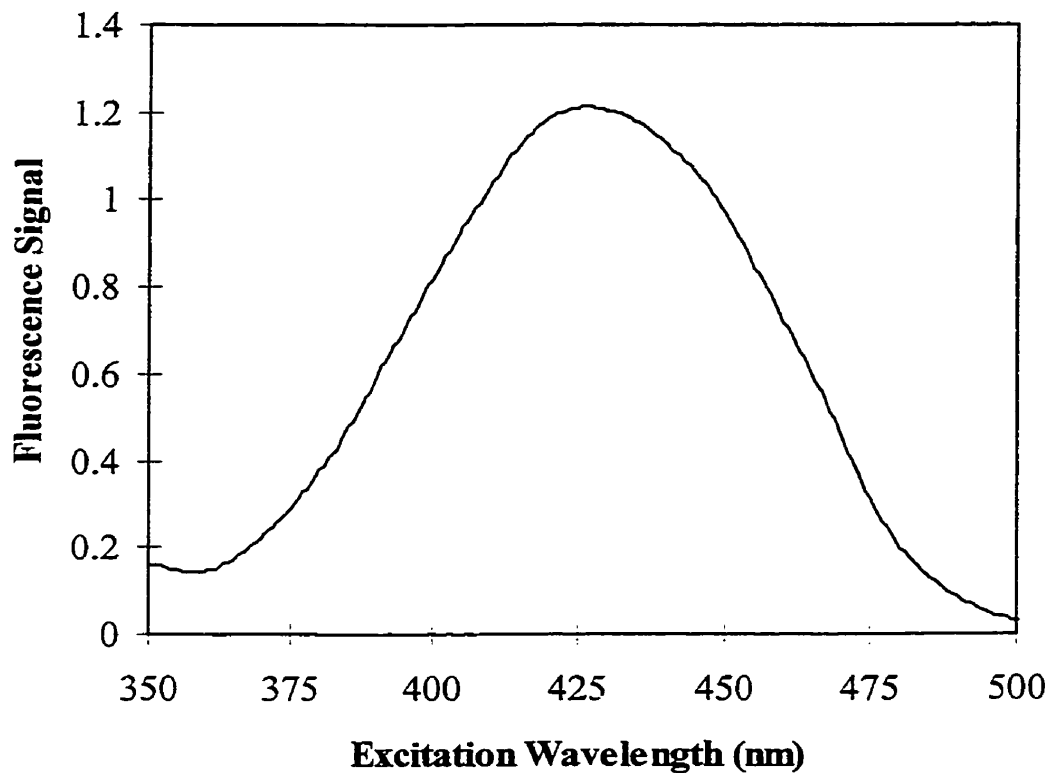
The potential interference of other natural water constituents with the fluorescence measurements has not been properly assessed and would be an important factor to take into consideration. Particulate matter present in natural waters may cause light scattering and a filtration step prior to fluorescence analysis may need to be considered. However, owing to the simple nature of fluorescence instrumentation, and large reductions in equipment size resulting from the development and implementation of fiber optic cables, this technique does show significant promise for field use in the future.

REFERENCES

1. Lund, W., *Fresenius J. Anal. Chem.*, **1990**, *337*, 557-564.
2. Bruccoleri, A., Lepore, G. and Langford, C.H., In *Environmental Oxidants*, J. O. Nriagu and M.S. Simmons (Eds.), John Wiley and Sons Inc., **1994**, pp187-200.
3. Buffle, J., In *Complexation Reactions in Aquatic Systems: an Analytical Approach*, Horwood, Chichester, **1988**, pp.195-200.
4. Cook, R.L. and Langford, C.H., *Environ. Sci. Technol.*, **1998**, *32*, 719-725.
5. Leenheer, J.A., Wershaw, R.L. and Reddy, M.M., *Environ. Sci. Technol.*, **1995**, *29*, 399-405.
6. Leenheer, J.A., Brown, G.K., MacCarthy, P. and Cabaniss, S.E., *Environ. Sci. Technol.*, **1998**, *32*, 2410-2416.
7. Hering, H.G. and Morel, F.M.M., *Environ. Sci. Technol.*, **1988**, *22*, 1469.
8. Mak, M.K.S. and Langford, C.H., *Inorg. Chim. Acta*, **1983**, *70*, 237.
9. Olson, D.L., and Shuman, M.S., *Anal. Chem.*, **1983**, *55*, 1103.
10. Shuman, M.S., Collins, B.J., Fitzgerald, P.J. and Olson, D.L., in *Aquatic and Terrestrial Humic Materials*, R.F Christman and E.T. Gjessing (Eds.), Ann Arbor Science, Ann Arbor, MI, **1983**, pp 349-370.
11. Bonifazi, M., Pant, B.C. and Langford, C.H., *Environmental Technology*, **1996**, *17*, 885-890.
12. Lavigne, J.A., Langford, C.H. and Mak, M.K.S., *Anal. Chem.*, **1987**, *59*, 2616-2620.
13. Buffle, J., In *Complexation Reactions in Aquatic Systems: an Analytical Approach*, Horwood, Chichester, **1988**, pp. 37-40
14. Langford, C.H. and Gutzman, D.W., *Analytica Chimica Acta*, **1992**, *256*, 183-201.
15. Saar, R.A. and Weber, J.H., *Anal. Chem.*, **1980**, *52*, 2095-2100.
16. Cook, R.L. and Langford, C.H., *Anal. Chem.*, **1995**, *67*, 1901-1908.

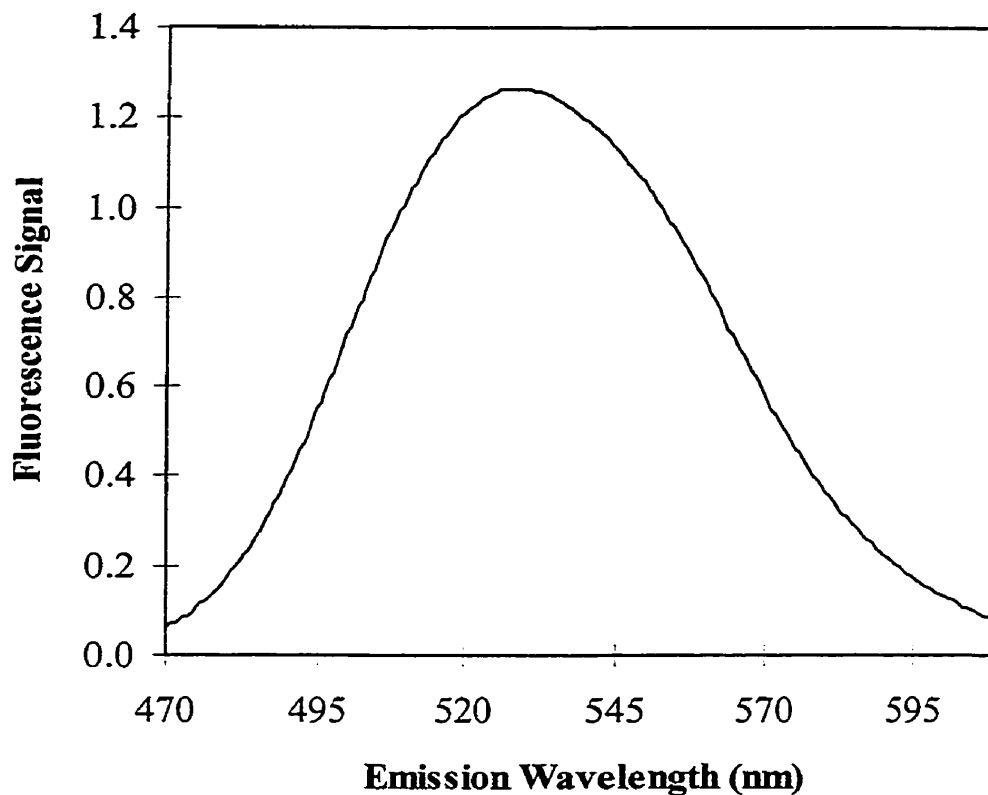
17. Gutzman D.W. and Langford, C.H., *Analytica Chimica Acta*, **1993**, *283*, 773-783.
18. Kalsbeck, W.A. and Thorpe, H.H., *J. Am. Chem. Soc.*, **1993**, *115*, 7146-7151.
19. Cook, R.L. and Langford, C.H., *Analyst*, **1995**, *120*, 591-596.
20. Lakowicz, J.R., *Principles of Fluorescence Spectroscopy*, Plenum Press, New York, **1983**, Chapter 9, 260-267.
21. Lavigne, J.A., PhD Thesis, Concordia University, Montreal, 1988.
22. Castanho, M.A.R.B. and Prieto, M.J.E., *Biochimica et Biophysica Acta*, **1998**, *1373*, 1-16.
23. Griffith, S.M., Schnitzer, M., *Soil Soc.*, **1975**, *120*, 126-131.
24. Schnitzer, M., Skinner, M., *Soil Soc.*, **1968**, *105*, 392-396.
25. Wang, Zd., Pant, B.C., and Langford, C.H., *Anal. Chim. Acta*, **1990**, *232*, 43-49.
26. Wang, Zd., Gamble, D.S., and Langford, C.H., *Environ. Sci. Technol.*, **1992**, *26*, 560-565.
27. Wang, Zd., PhD Thesis, Concordia University, Montreal, 1989.
28. Bruccoleri, A., Pant, B.C., Sharma, D.K. and Langford, C.H., *Environ. Sci. Technol.*, **1993**, *27*, 889-894.
29. Cook, R.L., Langford, C.H., Yamdagni, R. and Preston, C.M., *Anal. Chem.*, **1996**, *68*, 3979-3986.
30. Harris, D.C., *Quantitative Chemical Analysis*, 3rd Ed, W.H. Freeman and Co., New York, **1991**, 195-198.
31. Gamble, D.S., and Schnitzer, M., *Trace Metals and Metal Organic Interactions in Natural Waters*, P.C. Singer (Ed.), Ann Arbor Science Publications, Ann Arbor, Mich., **1973**, Chapter 9.
32. Schnitzer, M. and Khan, S.U., *Humic Substances in the Environment*, Marcel Dekker, New York, **1972**.

33. Langford, C.H., In *Ionic Interactions*, Vol. 2, S. Petrucci (Ed.), Academic Press, New York, 1971, p16.
34. Gamble, D.S, Underdown, A.W. and Langford, C.H., *Anal. Chem.*, 1980, 52, 1901-1908.

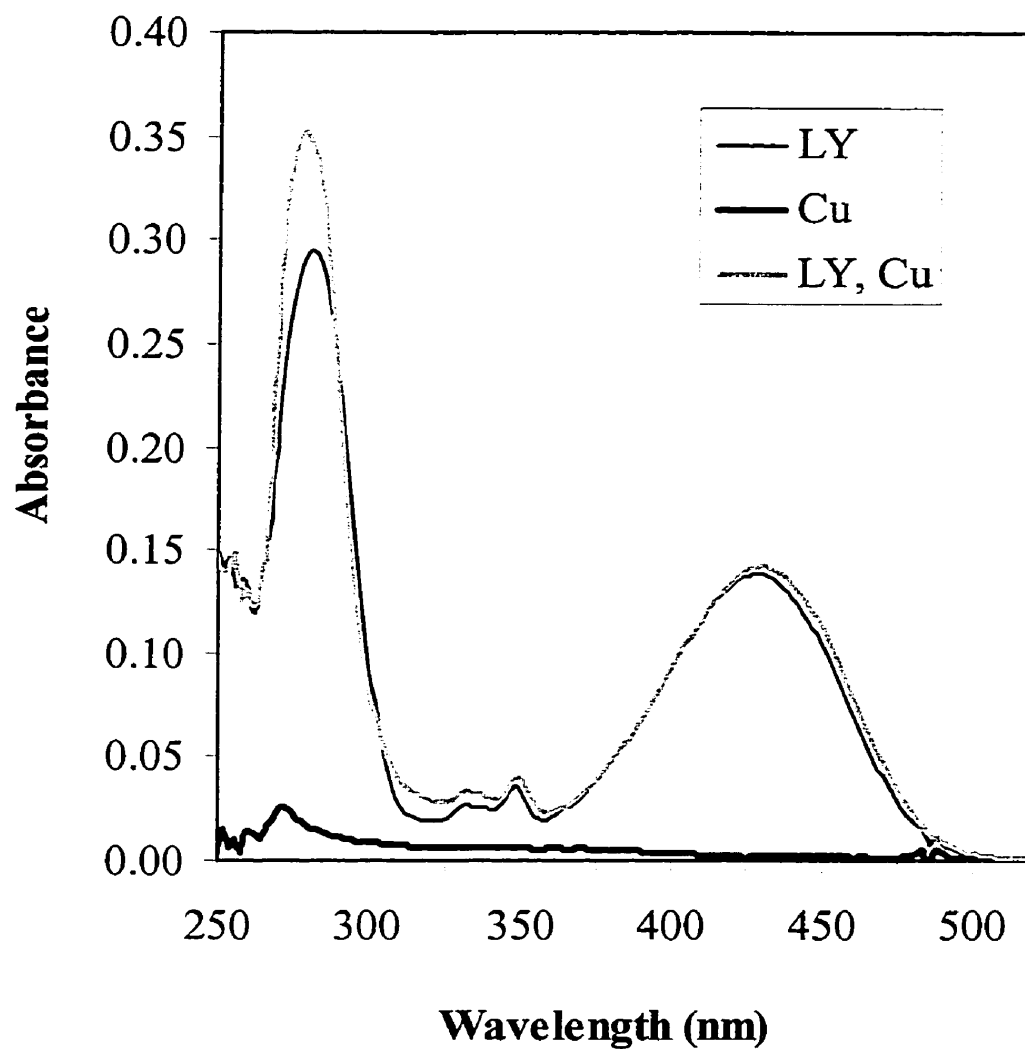
APPENDICES**Appendix 1** Fluorescence excitation spectrum for *Lucifer Yellow* fluorescent dye.

The fluorescence emission signal of a 0.87 μM solution of *Lucifer Yellow* dye in deionised water was monitored at 537 nm. The excitation wavelength was scanned over the range 350 – 500 nm. Maximum fluorescence excitation intensity was found at 428 nm.

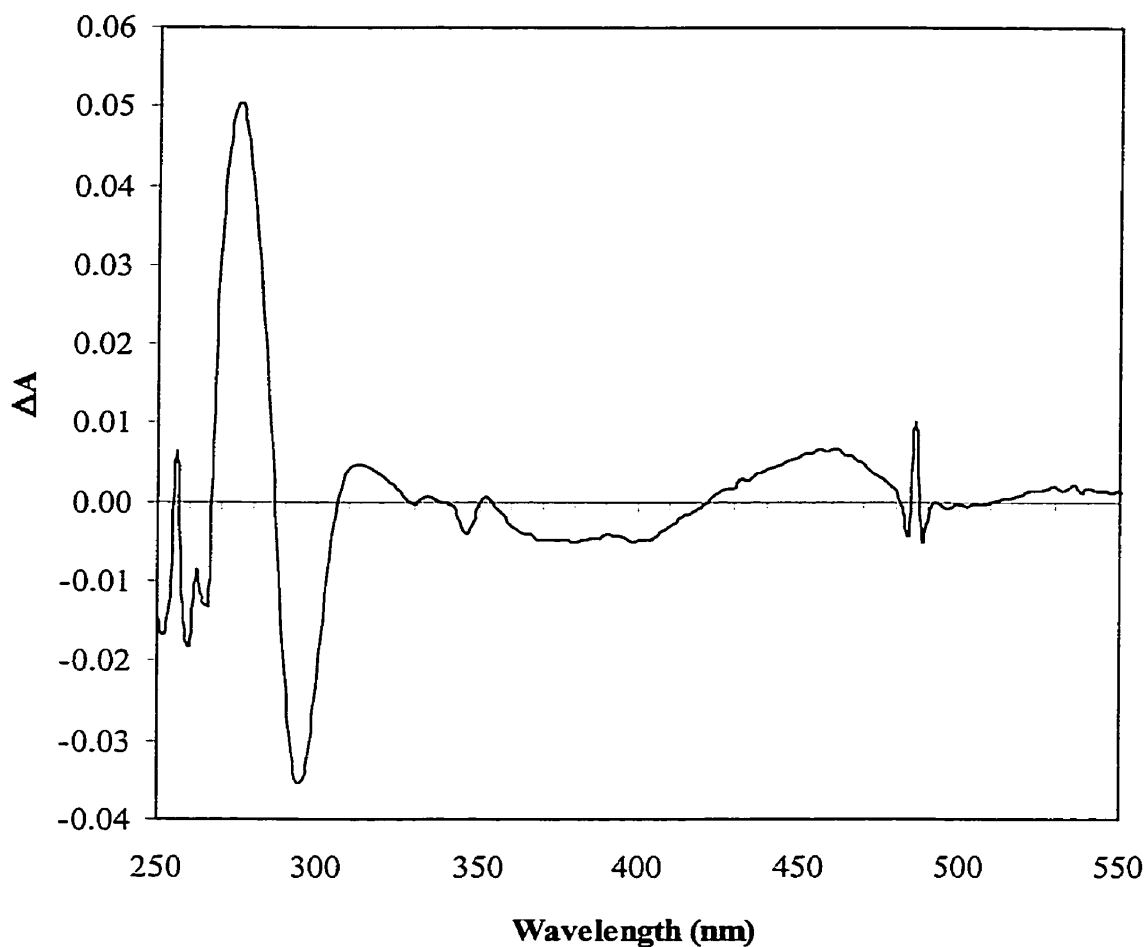
Appendix 2 Fluorescence emission spectrum for *Lucifer Yellow* fluorescent dye.



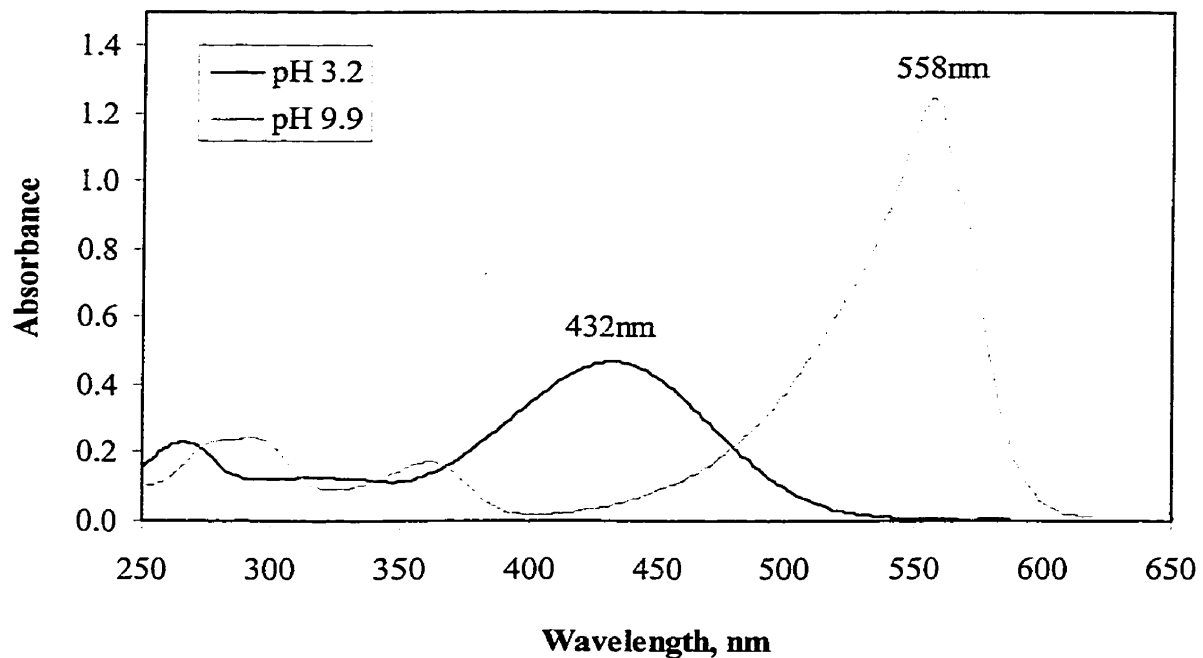
An 0.87 μM solution of Lucifer Yellow dye in deionised water was excited at 428 nm and the fluorescence emission signal was monitored over the wavelength range 470 – 610 nm. Maximum fluorescence emission intensity was found at 537 nm.

Appendix 3 Absorbance Spectra for LYD and Copper (II)

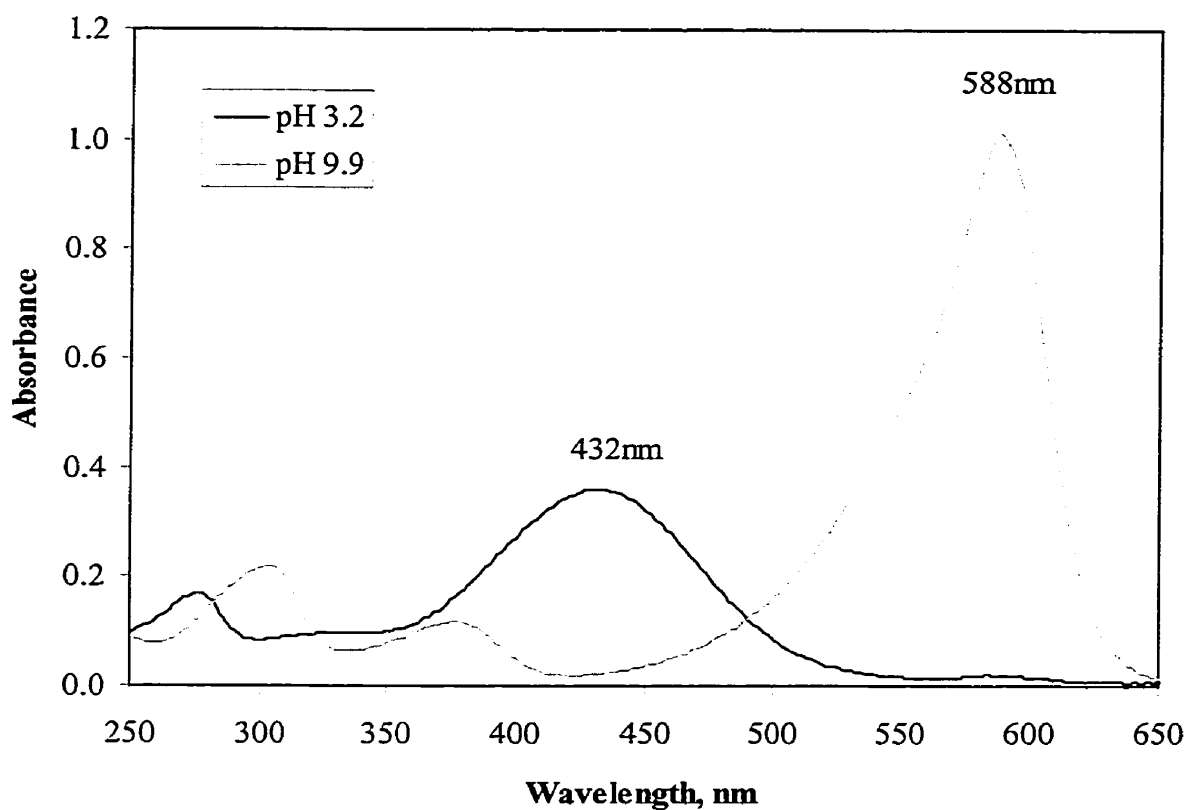
The absorbance spectra of LYD solution alone (11.9 μM), Cu^{2+} solution alone (1.51 mM) and a solution containing both LYD and Cu^{2+} (11.9 μM , 1.51 mM) were recorded. The curves were labeled as “LY”, “Cu” and “LY, Cu” respectively.

Appendix 4 Absorbance Difference Spectrum for LYD and Copper (II)

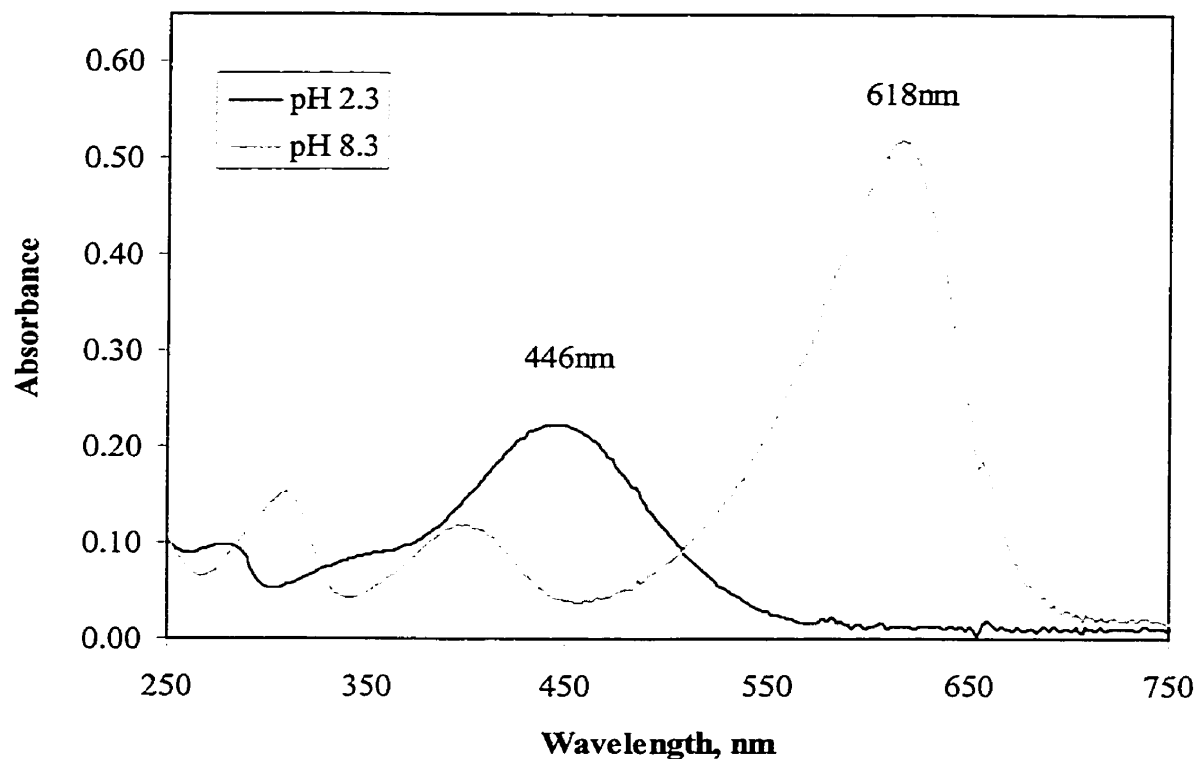
The absorbance difference (ΔA) spectrum of LYD solution alone (11.9 μM) plus Cu^{2+} solution alone (1.51 mM) and a solution containing both LYD and Cu^{2+} (11.9 μM , 1.51 mM). The individual LYD and Cu^{2+} spectra were added together and the combined result was subtracted from the spectrum of a solution containing both LYD and Cu^{2+} . $\Delta A = (\text{"LY"} + \text{"Cu"}) - (\text{"LY, Cu"})$

Appendix 5 Absorbance Spectra for *Phenol Red* pH Indicator Dye.

Absorbance spectra of 7.84 mg/L *Phenol Red* pH indicator dye at pH 3.2 and 9.9. The conjugate acid showed an absorbance maximum at 432 nm and the conjugate base had an absorbance maximum at 558 nm. The absorption coefficients for the conjugate acid at base forms at these wavelengths were calculated to be ϵ (acid, 432nm) = 0.0601 L mg⁻¹ cm⁻¹ and ϵ (base, 588nm) = 0.159 L mg⁻¹ cm⁻¹.

Appendix 6 Absorbance Spectra for *Bromocresol Purple* pH Indicator Dye.

Absorbance spectra of 7.84 mg/L *Bromocresol Purple* pH indicator dye at pH 3.2 and 9.9. The conjugate acid showed an absorbance maximum at 432 nm and the conjugate base had an absorbance maximum at 588 nm. The absorption coefficients for the conjugate acid at base forms at these wavelengths were calculated to be ϵ (acid, 432nm) = 0.0458 L mg⁻¹ cm⁻¹ and ϵ (base, 588nm) = 0.129 L mg⁻¹ cm⁻¹.

Appendix 7 Absorbance Spectra for *Bromocresol Green* pH Indicator Dye.

Absorbance spectra of 7.84 mg/L *Bromocresol Green* pH indicator dye at pH 2.3 and 8.3. The conjugate acid showed an absorbance maximum at 446 nm and the conjugate base had an absorbance maximum at 618 nm. The absorption coefficients for the conjugate acid at base forms at these wavelengths were calculated to be ϵ (acid, 432nm) = 0.0285 L mg⁻¹ cm⁻¹ and ϵ (base, 588nm) = 0.0658 L mg⁻¹ cm⁻¹.